Current Research in Food Science 10 (2025) 100977

Contents lists available at ScienceDirect

Current Research in Food Science

journal homepage: www.sciencedirect.com/journal/current-research-in-food-science

Trichosanthes kirilowii Maxim. Polysaccharide attenuates diabetes through the synergistic impact of lipid metabolism and modulating gut microbiota

Qiaoying Song , Kunpeng Zhang *, Shuyan Li , Shaoting Weng

College of Biotechnology and Food Science, Anyang Institute of Technology, Huanghe Road, Anyang, 455000, China

ARTICLE INFO

Handling Editor: Dr. Yeonhwa Park

Keywords:
Trichosanthes kirilowii maxim.
Polysaccharide
T2DM

ABSTRACT

Polysaccharide, a chain of sugars bound by glycosidic bonds, have a wide range of physiological activities, including hypoglycemic activity. In present study, we established T2DM mice models to explore the effects and mechanism of *Trichosanthes kirilowii* Maxim polysaccharide (TMSP1) on high-fat diet/streptozotocin (HF-STZ) induced diabetes mice. The results showed that high-fat diet significantly increased the oral glucose tolerance test (OGTT), viscera index, oxidative stress, impaired glucose tolerance, decreased body weight, immune response and short-chain fatty acid (SCFAs) content, and disrupted the balance of intestinal flora structure. However, after 6 weeks of TMSP1 intervention decreased lipid accumulation, ameliorated gut microbiota dysbiosis by increasing SCFAs-producing bacteria and mitigated intestinal inflammation and oxidative stress. Moreover, TMSP1 significantly restored the integrity of the intestinal epithelial barrier and mucus barrier. The results of fecal microbiota transplantation confirmed that TMSP1 exerted hypoglycemic effect through regulating intestinal flora to a certain extent. Collectively, the findings revealed TMSP1 intervention inhibits hyperglycemia by improving gut microbiota disorder, lipid metabolism, and inflammation. Hence, TMSP1 may be an effective measure to ameliorate HF-STZ induced diabetes.

1. Introduction

Trichosanthes kirilowii Maxim. has received more and more attention from scholars due to its significant medical value (Liang et al., 2009). On April 16, 2010, Anyang *Trichosanthes kirilowii* Maxim was approved by the Ministry of Agriculture of the People's Republic of China as a geographical indication registration protection product for agricultural products, and the approval number is Announcement No. 1374 of the Ministry of Agriculture. In 2022, the Health Commission of the People's Republic of China approved the seed of *Trichosanthes Kirilowii* as a new food raw material. Modern medical studies have confirmed that *Trichosanthes kirilowii* Maxim. Rich in nutrients such as unsaturated fatty acids, protein, amino acids (Abbou et al., 2019). Therefore, *Trichosanthes kirilowii* Maxim., known as "drug homologous food", have been used widely to cure various diseases, such as diabetes, cancer and heart disease. At present, the research on *Trichosanthes kirilowii* Maxim. mainly focused on flavonoids, essential oils, proteins (Wang et al., 2009; Rahman and Moon, 2007; Moon et al., 2008; Shu et al., 2009). In the meantime, the researches on *Trichosanthes kirilowii* Maxim polysaccharide mainly focused on the peel and seeds. Jing and his collaborators have shown that polysaccharide from the peel of *Trichosanthes kirilowii* Maxim presented anti-hyperlipidemia activity (Jing et al., 2024). Hu's research showed the immunomodulatory activity on RAW264.7 cells of polysaccharides from *Trichosanthes kirilowii* Maxim seeds (Hu et al., 2020).

Polysaccharides are extensive chains of monosaccharide units interconnected by glycosidic bonds, comprising at least ten such units (Liu et al., 2021a). These compounds are widely recognized in nature for their crucial physiological functions, which include bacteriostatic properties, hypoglycemic effects, reduction of blood pressure, and anti-tumor activities (Liu et al., 2021b; Barbosa and Junior, 2021; Wang et al., 2022a).

Type 2 diabetes mellitus (T2DM) is a metabolic disorder defined by elevated blood glucose levels, which arise from either inadequate secretion of insulin or the development of insulin resistance (Moheet et al., 2015). Diabetes mellitus is widely recognized as a condition characterized by intricate metabolic disorder mechanisms, encompassing disturbances in carbohydrate, lipid, and protein metabolism (Guan et al., 2016). The International Diabetes Federation (IDF) has released a report from the International Diabetes Program, forecasting that by

* Corresponding author.
E-mail address: zhangkunpengag@163.com (K. Zhang).

https://doi.org/10.1016/j.crfs.2025.100977
Received 3 September 2024; Received in revised form 8 January 2025; Accepted 16 January 2025
Available online 19 January 2025
2665-9271/© 2025 The Authors. Published by Elsevier B.V. This is an open access article under the CC BY-NC-ND license (http://creativecommons.org/licenses/by-nc-nd/4.0/).

2040, approximately 642 million individuals worldwide will be living with diabetes, with China projected to have the highest prevalence. This indicates a substantial increase in global cases over a relatively brief period when compared to previous evaluations of diabetes prevalence (Li et al., 2019). It is alarming that diabetes can result in a range of long-term complications, such as diabetic nephropathy, hepatitis, hypertension. As diabetes advances, the complexities it introduces can become progressively more difficult to manage. Consequently, prompt identification and proactive interventions are essential for mitigating and potentially treating the condition. Simultaneously, excessive fat accumulation in patients with T2DM can trigger inflammatory and oxidative stress responses, leading to pathological alterations in the liver. Furthermore, diabetes induces renal damage through abnormal hemodynamic changes and metabolic dysregulation (Miao et al., 2019).

It is generally accepted that the interaction between lipid levels and type 2 diabetes is complex. First, when blood lipid concentrations are elevated, especially low density lipoprotein (LDL) and total cholesterol, this leads to narrowing and stiffness of blood vessels. In contrast, diabetes can have an adverse effect on blood lipids (Wang et al., 2015). Impaired insulin secretion and action will cause diabetes. And diabetes is linked with dyslipidemia as well. When insulin is insufficient or dysfunctional, the balance between fat production and lipolysis is disrupted, potentially leading to elevated lipid levels. Therefore, there is a significant causal relationship between lipid levels and diabetes (Li et al., 2021). For people with diabetes, controlling lipid levels is especially important to reduce the risk of cardiovascular disease.

The composition and functionality of intestinal microflora, along with its bioactive metabolites, are crucial for sustaining human intestinal health (Zhang et al., 2020a). They supplied essential nutrients and energy to the host by fermenting indigestible dietary components within the large intestine, thereby promoting metabolic equilibrium and enhancing immune system balance in the host (Brian K et al., 2005). Research indicates that the composition of intestinal microbiota exhibits fluctuations within a specific range, influenced by various factors including environmental conditions, age, physiological status, and dietary habits (Wang et al., 2007). The dysbiosis of intestinal microbiota not only precipitates infections and inflammation within the gastrointestinal tract but also significantly elevates the risk of chronic conditions such as diabetes, obesity, and gastrointestinal cancers (Giuliano et al., 2015). As individuals age, the equilibrium of intestinal microbiota is disrupted, leading to a decline in beneficial bacteria, particularly those dominated by Gram-positive species such as *Bifidobacterium*, while harmful bacteria proliferate (Bao et al., 2014). Meanwhile, several scholars had posited that intestinal microbiota played a crucial role in various metabolic processes within the human body, including nutrient absorption, energy homeostasis, and glucose and lipid metabolism. Furthermore, dysbiosis of the intestinal microbiota was closely associated with the onset, progression, and outcomes of metabolic disorders such as type 2 diabetes (Kyrgiou et al., 2017). Qin Junjie demonstrated that individuals with type 2 diabetes exhibited a moderate dysbiosis of the intestinal microbiota, primarily characterized by a reduction in beneficial bacterial populations within the gut, such as butyrate-producing bacteria, while there was a significant increase in various opportunistic pathogenic bacteria (Qin et al., 2012). Furthermore, in the pathological condition of diabetes, the excessive production of endotoxins was released into the bloodstream, triggering a systemic non-specific inflammatory response that promotes insulin resistance and exacerbates abnormal glucose metabolism (Plovier et al., 2016).

Consequently, this study aimed to investigate the hypoglycemic effects of *Trichosanthes kirilowii* Maxim. polysaccharide in high-fat/STZ-induced C57BL/6J diabetic mice. Additionally, the underlying mechanisms of the hypoglycemic action of the polysaccharide were elucidated through an analysis of lipid metabolism and intestinal microbiota, thereby providing theoretical support for the therapeutic application of *Trichosanthes kirilowii* Maxim.

2. Materials and methods

2.1. Strain and reagents

The *Trichosanthes kirilowii* Maxim. used in this study was provided by the College of Biotechnology and Food Science at Anyang Institute of Technology. Chloroform, n-butanol, Sephadex-150, phenol, sulfuric acid, and streptozotocin were purchased from Sigma Chemical Co. (St. Louis, MO, USA). Acarbose was sourced from Bayer. ELISA kits for glutathione peroxidase (GSH-Px), superoxide dismutase (SOD), malondialdehyde (MDA), fasting serum insulin (FINS), total bilirubin (TBIL), fasting insulin (FIns), insulin C-peptide (C-P of INS), glycosylated hemoglobin (GHb1Ac), glycogen, free fatty acids (FFA), phosphoenolpyruvate carboxykinase (PEPCK), hexokinase (HK), glucose-6-phosphatase (G-6-Pase), tumor necrosis factor α (TNF-α), interleukin-6 (IL-6), interleukin-10 (IL-10) and interleukin −12 (IL -12) were obtained from Nanjing Jiancheng Biotechnology Co., LTD. All other chemicals used in this research were of analytical grade.

Healthy male C57BL/6J mice (5 weeks old, weighing 20 ± 2 g) were obtained from Sibeifu Biotechnology Co., Ltd. (Beijing, China). All animal care and experimental procedures followed the guidelines of the US National Institutes of Health (NIH Publication No. 85–23, revised 1996). No human subjects were involved in any of the experiments. The research was approved by the Institute of Radiation Medicine, Chinese Academy of Medical Science under approval number IRM-DWLL-2022250.

2.2. Preparation of polysaccharide

The study utilized polysaccharides extracted from *Trichosanthes kirilowii* Maxim. through a process of water extraction and subsequent alcohol precipitation (Li and Huang, 2021). The dried *Trichosanthes kirilowii* Maxim. powder (1 g) was added into the distilled water (30 mL) to extract polysaccharides at 80 °C for 2 h. Subsequently, the supernatant was precipitated using 80% ethanol. Following this, the Sevag reagent (Chloroform: n-butanol = 4:1) was employed to eliminate proteins from the sample, thereby yielding crude polysaccharide (C-TMSP). Finally, homogeneous polysaccharide (TMSP1) was isolated utilizing a Sephadex-150 column (40 cm × 1.6 cm) (Zhou et al., 2021). The molecular weight of TMSP1 was determined to be 690.239 kDa. Moreover, TMSP-1 was composed of six sugar alcohol derivatives: →3)-D-Galp-(1→, D-Glcp-(1→, →4)-D-Manp-(1→, →6)-D-Galp-(1→, →4)-D-Galp-(1→, and →4,6)-D-Manp-(1 → . The chemical structure and chemical formula of TMSP1 was shown in Fig. 1(A) and (B). Additionally, the sugar content of TMSP1 was quantified using the Phenol-sulfuric acid method (Yan et al., 2019).

2.3. Animal experiment 1

To examine the impact of TMSP1 on blood glucose homeostasis in mice, a total of 20 mice were allocated into two groups: the normal group (NG, n = 10) and the experimental group (EG, n = 10). The NG group of mice was administered a normal diet and sterile water freely for 10 weeks. In contrast, the EG group of mice received a normal diet and underwent intragastric administration of TMSP1 at the same dosage (100 mg/kg/day) daily for 10 weeks (SFig. 1). Throughout the experiment, the body weight and fasting blood glucose (FBG) levels of the mice were assessed on a weekly basis. Following a 10-week feeding period, serum samples from each group of mice were collected for the analysis of serum metabolic indices (Li et al., 2023).

2.4. Animal experiment 2

All C57BL/6J mice were acclimatized for one week prior to the onset of type 2 diabetes. The parameters for adaptive feeding include: humidity levels maintained at 45–55%, temperature regulated between 23

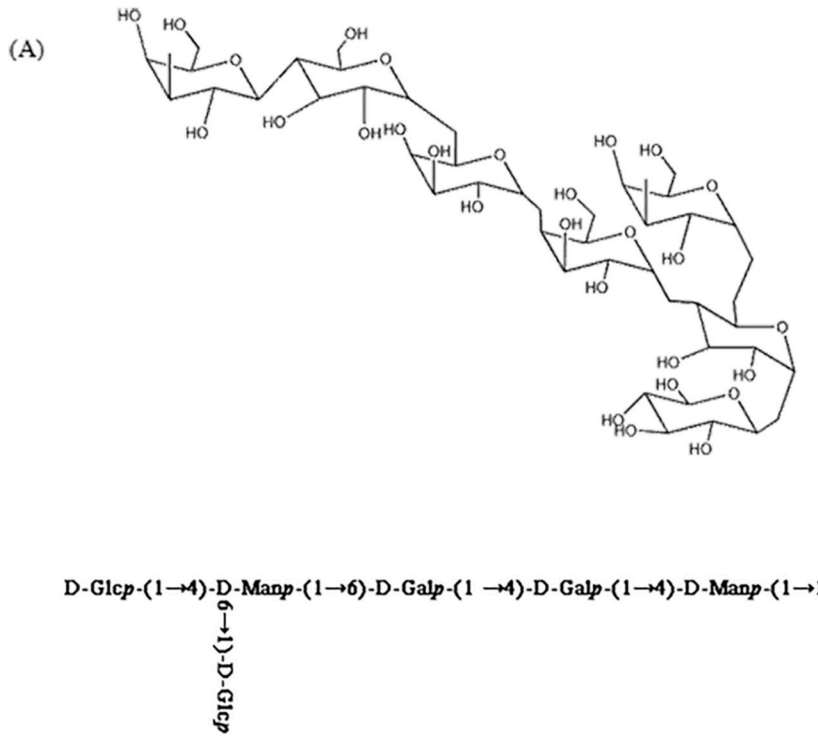

Fig. 1. The chemical structure of TMSP1. The chemical formula of TMSP1 was $C_{42}H_{72}O_{36}$. (TMSP1: *Trichosanthes kirilowii M*axim. homogeneous polysaccharide).

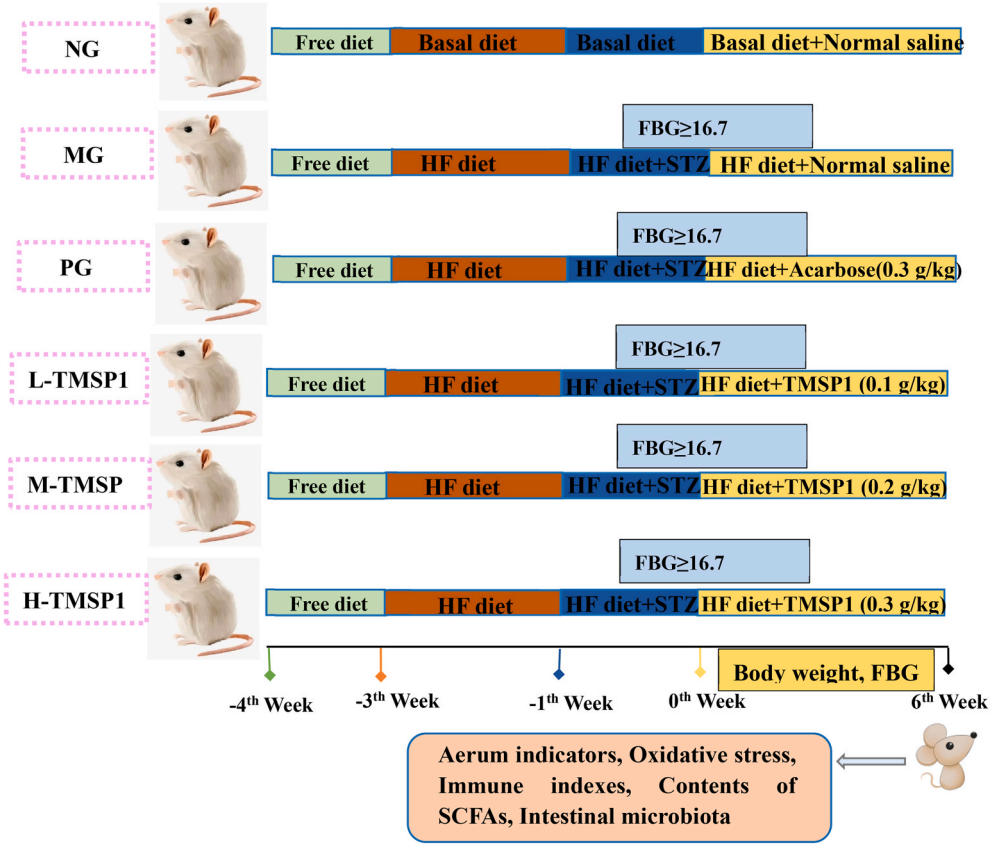

Fig. 2. Schematic representation of the modeling and treatment protocols in animal experimentation. (TMSP1: *Trichosanthes kirilowii M*axim. homogeneous polysaccharide, NG: normal group, MG: mellitus control group, PG: Positive Control Group, L-TMSP1: low dose TMSP1, M-TMSP1: middle dose TMSP1, H-TMSP1: high dose TMSP1, SCFAs:short-chain fatty acid, HF: high-fat diet, STZ: streptozotocin, FBG: fasting blood glucose).

and 25 °C, and light-dark cycles of 12 h each (Goyal et al., 2016). Following the adaptive feeding phase, mice in the normal group (NG group, n = 10) were provided with a basal diet every day, whereas mice in the other groups received a high-sugar and high-fat diet every day for two weeks, comprising 40% fat, 42% carbohydrates, and 18% protein for a duration of two weeks. Subsequently, a daily intraperitoneal injection of 40 mg/kg/d STZ (dissolved in citrate buffer at pH 4.2–4.4) was administered to C57BL/6J mice, excluding the NG group, for a duration of one week. The diabetic mouse model can be deemed successfully established if the fasting blood glucose (FBG) levels exceed 16.7 mmol/L (Liang et al., 2020). The diabetic mice were randomly divided into 5 groups: diabetes mellitus control group (MG, administration of 1 mL/kg citric acid buffer solution), Positive Control Group (PG, High-sugar, high-fat diet +0.03 % Acarbose (300 mg/kg), n = 10), low dose TMSP1 (L-TMSP1, administration of High-sugar, high-fat diet +100 mg/kg TMSP1, n = 10) group, middle dose TMSP1 (M-TMSP1, administration of High-sugar, high-fat diet +200 mg/kg TMSP1, n = 10) group and high dose TMSP1 (H-TMSP1, administration of High-sugar, high-fat diet +300 mg/kg TMSP1, n = 10) group (Fig. 2) (Wang et al., 2017; Lang et al., 2020). The TMSP1 was delivered by intragastric administration once a day. During the feeding period, the body weight and fasting blood glucose (FBG) levels of the mice were recorded every seven days. Following six weeks of treatment, the mice underwent a 12-h fasting period. Subsequently, 1 h post-administration, each group of mice was administered a glucose solution at a dosage of 2.0 g/kg by intragastric administration. Blood was collected by tail tip sampling, and blood glucose levels were then measured at intervals of 20 min, 40 min, 60 min, 80 min, 100 min and 120 min, respectively. Following 28 days of administration, the mice were anesthetized via intraperitoneal injection of 2% pentobarbital sodium and subsequently euthanized through spinal dislocation. Serum was obtained by excising the eyeballs. The liver, kidneys, and cecum were harvested post-dissection, and organ indices were measured (Wu et al., 2022a).

2.5. Animal experiment 3

Prior to the fecal microbiota transplantation (FMT) experiment, all mice were accommodated for one week and subsequently administered antibiotics (rifaximin, 150 mg/kg/day) for an additional daily for 2 weeks. Subsequently, the mice were randomly allocated into two distinct groups: H-TMSP1-FMT (n = 5) group and MG-FMT group (n = 5). 40 mg/kg/d of STZ (dissolved in citrate buffer, pH 4.2–4.4) was injected intraperitoneally to the mice daily, until the FBG of mice determined with a fingertip glucose meter (G3-A, Dexcom) exceeded 16.7 mmol/L. Fecal samples from the MG group and H-TMSP1 group were collected separately and subsequently dissolved in 5 mL of normal saline. Subsequently, the mixture was subjected to centrifugation at 4000 rpm for 10 min to isolate the supernatant. The isolated supernatant was administered to recipient mice once daily for 8 weeks. At the same time, FBG levels of mice were assessed weekly. Subsequently, the mice in each group were euthanized, and then the cardiac blood biochemical indexes were collected for detection (SFig. 2).

2.6. Determination of serum indicators

Blood samples from the mice were collected prior to their sacrifice. Subsequently, serum was obtained by centrifugation at 2000 rpm for 20 min at 4 °C. The levels of aspartate aminotransferase (AST), albumin (ALB), blood urea nitrogen (BUN) and creatinine (CRE) were operated by using an automated biochemical analyzer (BK-400) respectively. The FINS, TBIL, FIns, C-P of INS, GHb1Ac, glycogen and FFA levels in each group were obtained by using the insulin ELISA kit (Wuhan Elabscience Company) (Wu et al., 2022b).

2.7. Oxidative stress analysis

The serum from each group was collected following the sacrifice of the mice. The enzyme activity of glutathione peroxidase (GSH-Px), superoxide dismutase (SOD) and the content of malondialdehyde (MDA) were measured by using the insulin ELISA kit (Cardullo et al., 2020a).

2.8. Detection of enzyme activity related to blood glucose metabolism

The enzyme activities of phosphoenolpyruvate carboxykinase (PEPCK), hexokinase (HK) and glucose-6-phosphatase (G-6-Pase) were assessed using specific Enzyme-Linked Immunosorbent Assay (ELISA) kits sourced from Nanjing Jiancheng, China (Wu et al., 2019; Chiang, 2009; Li et al., 2011).

2.9. Detection of serum immune indexes

The levels of Tumor Necrosis Factor-α (TNF-α), Interleukin-6 (IL-6), Interleukin-10 (IL-10), and Interleukin-12 (IL-12) were quantified using ELISA kits which was purchased from Biotechnology Inc. (Shanghai, China) (Fan et al., 2017a).

2.10. Determination of contents of SCFAs

Following the experiment, the chyme from the terminal segment of the cecum was collected and preserved at −80 °C. Short chain fatty acids (SCFAs) were analyzed using gas chromatography-mass spectrometry. The standard curves for each short-chain fatty acid were constructed using the internal standard method. A mixture of 300 μL of 50% sulfuric acid and 0.2 g of chyme was introduced into a solution containing the internal standard, cyclohexanone (500 mg/L, 100 μL), and subsequently centrifuged at 12,000 rpm for 10 min. The supernatant was then collected for the analysis of SCFAs content. The chromatographic separation was performed using an Agilent DB-WAX capillary column (30 m × 0.25 mm × 0.25 μm). Carrier gas: high purity helium (purity ≥99.999%); Carrier gas flow rate: 1.0 mL/min; Inlet temperature: 220 °C; Injection size: 1 μL, no shunt injection; The heating procedure is: 60 °C for 1 min, rise to 210 °C at 30 °C/min for 3 min. Ion source: EI, ion source temperature 230 °C, interface temperature 220 °C (Hu et al., 2019; Chen et al., 2020a).

2.11. Histopathological analysis

The pancreas, colon, liver and kidney of the mice were preserved in 10% paraformaldehyde quickly after the mice sacrificed. Then, the sample were dehydrated by using a range of different concentrations of ethanol. After that, the above sample were sliced with a slicer after waxdiped and embedded. In addition, hematoxylin and eosin (H&E) staining method was operated whereafter. The microscope was used for observation of the histopathological ultimately (Tong et al., 2006). The pathological scores of liver were measured by Schmidt Pathology Scale. The score was based on the degree of tissue edema, necrotic area, bleeding and inflammatory cell infiltration. Otherwise, the renal H&E stained slides were scored based on the following criteria: (a) no tubular injury = 0, (b) minor injury (damaged renal tubules accounted for less than 5% of total renal tubules) = 1, (c) mild injury (damaged renal tubules accounted for 5%–25% of total renal tubules) = 2, (d) Moderate injury (damaged renal tubules accounted for 25%–75% of the total renal tubules) = 3, (e) severe injury (damaged renal tubules accounted for >5% of the total renal tubules) = 4 points. The higher the score, the more severe the damage.

2.12. Immunofluorescence staining

Paraffin sections of colon tissue were taken from each group of mice, dewaxed with xylene, fixed with acetone for 10 min, washed with

phosphate buffered saline (PBS). Subsequently, goat serum was sealed and incubated in a room temperature wet box in dark for 30 min. The primary antibody (dilution 1:100) was added and incubated overnight in a humidified chamber at 4 °C in dark. Subsequently, following a wash with PBS, a fluorescent secondary antibody was introduced and incubated in a humidified chamber at 37 °C for 1 h in dark. Following a subsequent wash with PBS, the nucleus was stained with 2-(4-Amidinophenyl)-6-indolecarbamidine dihydrochloride (DAPI) for 5–10 min, and the slide was then sealed.

2.13. Intestinal microbiota analysis

The cecum was collected after the mice sacrificed. The nucleic acid extraction and purification reagent DNA kit (Omega Bio-tek, Norcross, GA, U.S) was used for DNA extraction, and determined the quantity and quality of DNA (Caporaso et al., 2010; Gill et al., 2006). In addition, specific primers were used to amplify genes in different regions. The primer sequence used in this study were shown in Stable1. The QIIME software was employed to compute the OTU levels and assess alpha diversity indices, including Chao1, ACE, PD_whole_tree, Shannon, Simpson index. Beta diversity analysis was conducted by calculating the UniFrac distance measure using Qimme software, followed by the generation of PCA, PCoA, and NMDS diagrams (Rognes et al., 2016).

2.14. Statistics assay

The data were presented as the mean ± SD using Excel 2022. Experimental data are expressed as mean ± standard deviation. Differences between groups of rats were analyzed by one-way ANOVA using SPSS 27.0 software. Differences at $P < 0.05$ were considered significant. The 16S rRNA sequencing data were analyzed using the Wilcoxon rank-sum test to detect significant differences among groups.

3. Result and discussion

3.1. Preparation of polysaccharide

In this study, the crud polysaccharide obtained from *Trichosanthes kirilowii* Maxim. was purified with column of Sephadex 150 to obtain the homogeneous polysaccharide (TMSP1). As illustrated in Fig. 3, a single symmetrical peak was observed, indicating the homogeneity of TMSP1. The result of Phenol-sulfuric acid method showed that the sugar content of TMSP1 was 96.58%, thereby confirming its suitability for subsequent experimental applications.

3.2. Effect of TMSP1 on glucose homeostasis in C57BL/6J mice

To assess the impact of TMSP1 on blood glucose levels in mice, we initially conducted a 10-week oral administration of TMSP1 in normal C57BL/6J mice. The level of body weigth, FBG levels of mice weekly during the experiment, oral glucose tolerance test (OGTT), Hemoglobin A1c (HbA1C) and FBG in NG group and EG group were shown in Fig. 4. No significant differences were observed among these five parameters following 10 weeks of TMSP1 treatment. At the same time, the area under curves (AUC) of blood glucose showed no difference between NG and EG groups, indicating that long-term consumption of TMSP1 does not exert a notable impact on the blood glucose homeostasis in mice.

3.3. Ameliorative effect of TMSP1 on diabetic symptoms in T2DM rats

The data presented in Fig. 5(A) indicated that the administration of TMSP1 did not result in statistically significant changes in body weight among diabetic mice after a two-week treatment period ($p > 0.05$). From the third week of polysaccharide intervention, a significant decrease in the weight of mice in the MG group was observed, demonstrating a noticeable difference compared to the other groups ($p < 0.05$). Weight loss is commonly observed in individuals with type 2 diabetes, indicating the successful development of a diabetic mouse model (Chen et al., 2020b). In addition, the mice in the PG group exhibited a significant increase in body weight compared to those in the MG group ($p < 0.05$). Furthermore, weekly blood glucose levels of the mice in each group were monitored during polysaccharide treatment. As illustrated in Fig. 5 (B), the blood glucose levels of mice in the NG group consistently remained within the range of 7–8, indicating that these mice maintained euglycemia. Three weeks prior to the initiation of polysaccharide treatment, there were no significant differences in blood glucose levels among the MG, PG, L-TMSP1, M-TMSP1 and H-TMSP1 groups. However, starting from the fourth week of polysaccharide treatment, the blood glucose levels of mice in the PG, L-TMSP1, M-TMSP1 and H-TMSP1 groups exhibited a decrease compared to those in the MG

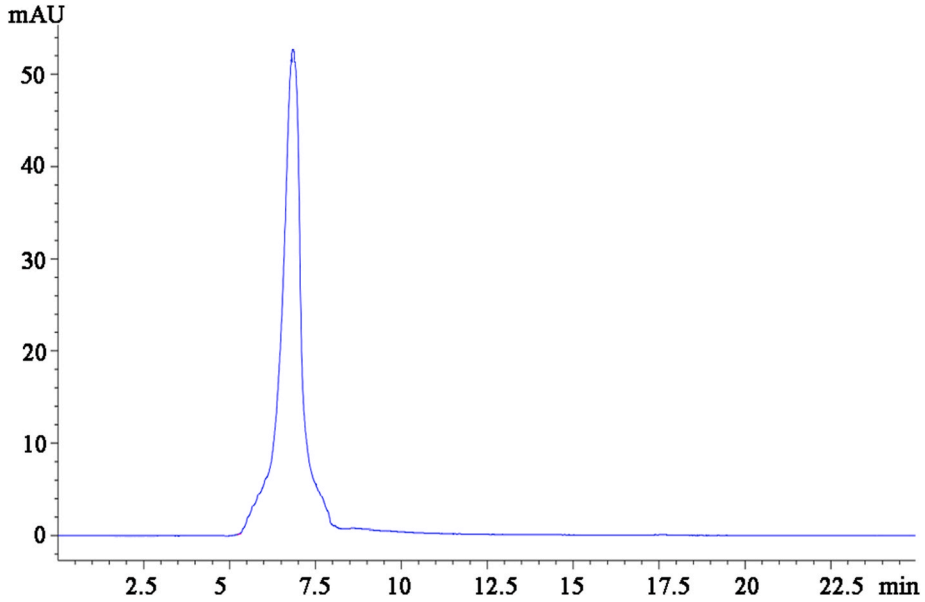

Fig. 3. The weight-average molecular weight (Mw) of TMSP1. The single symmetrical peak indicated the homogeneity of TMSP1. (TMSP1: *Trichosanthes kirilowii Maxim.* homogeneous polysaccharide).

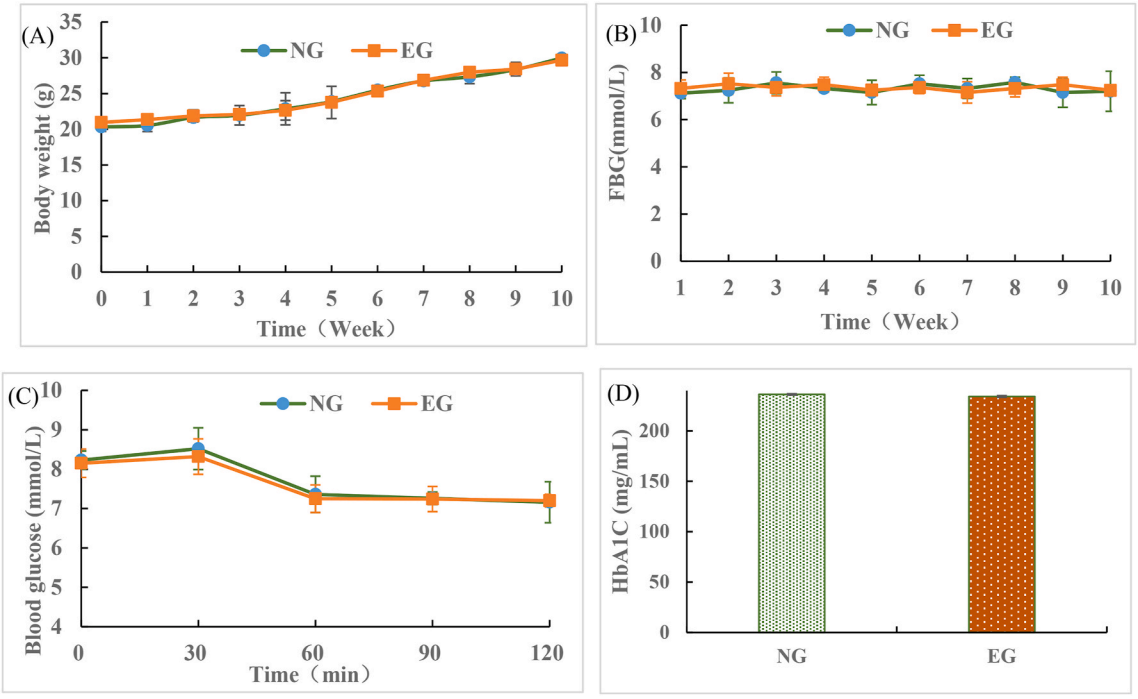

Fig. 4. There were no significant differences in (A) body weight and (B) FBG levels of mice weekly during the experiment among the groups each week. After feeding for 10 weeks, there was no significant difference in (C) blood glucose and (D) HbA1C. NG group mice were given normal diet and sterile water at a dose of 100 mg/kg/day, and EG group mice were given normal diet and gavage the same dose of TMSP1 (100 mg/kg/day) every day for 10 weeks. Data are presented as means ± SEM (n = 10). Values denoted by different letters indicate significant differences ($P < 0.05$). (TMSP1: *Trichosanthes kirilowii M*axim. homogeneous polysaccharide, NG: normal group, EG: experimental group, FBG: fasting blood glucose, HbA1C:Hemoglobin A1c).

group ($p < 0.05$). Additionally, mice in the MG group consistently displayed elevated blood sugar levels. In addition, compared with MG group (2093.3 mmol/L·min), AUC of blood glucose was significantly decreased in L-TMSP1 (2052.9 mmol/L·min), M-TMSP1 (1887.3 mmol/L·min) and H-TMSP1 (1756 mmol/L·min) groups.

The liver and kidney index results for the mice in each group were presented in Fig. 5(C). It is apparent from the figure that the organ index of mice in the MG group showed a statistically significant increase compared to the other groups ($p < 0.05$). The elevation of blood sugar levels disrupted the metabolism of sugar and lipids, leading to increased hepatic fat accumulation (Fu et al., 2021). Moreover, diabetic mice displayed kidney edema, resulting in a significant increase in kidney index (Zeng et al., 2023). After the TMSP1 intervention, there was a significant decrease in the organ index of the three sample groups compared to the MG group ($p < 0.05$). However, there was still a notable difference with the NG group ($p < 0.05$), while no significant variance in organ index was observed between the PG group and NG group ($p > 0.05$).

The regulation effect of *Trichosanthes kirilowii* Maxim. Polysaccharide on blood glucose level suggested its potential to ameliorate pancreatic pathology. In the NG group, as depicted in Fig. 5(D), the pancreatic tissue exhibited completeness, with a full islet structure and closely arranged intact β cells. The boundary between islets and exocrine glands was clearly defined. In the MG group, the islet structure exhibited incompleteness, nearly damaged beta cells, and abnormal cell morphology. Additionally, non-uniform islet boundaries and vacuolar infiltration in the interior were observed. The relatively intact islets also displayed a trend of atrophy, indicating that a high-sugar and high-fat diet imposed a significant burden on and caused damage to the pancreas of diabetic mice. After polysaccharide intervention, the pathological morphology of pancreatic tissue showed a significant reduction, with intact islets closely resembling those of the control group. The β cells within the islets were relatively densely arranged. Additionally, there was an improvement in internal cavity infiltration phenomenon, resulting in clearer islet morphology and a plumper structure compared to the MG group. The findings suggested that *Trichosanthes kirilowii* Maxim. Polysaccharide has the potential to ameliorate the pancreatic pathological conditions induced by a high sugar and high fat diet in rats, thereby alleviating pancreatic burden and preventing islet atrophy.

The level of serum insulin during fasting, known as FIns, primarily reflects the normal basal insulin level required to maintain fasting blood glucose. Elevated FIns levels may indicate impaired islet cell function or insulin resistance. C-peptide is a peptide fragment cleaved from endogenous insulin, serving as an indicator of endogenous islet function. In cases of insulin resistance or decreased insulin sensitivity, excessive C-peptide secretion occurs in order to lower blood sugar levels, leading to elevated C-peptide levels. HbA1c is a compound formed by the binding of glucose to hemoglobin in human blood, serving as a crucial indicator for diagnosing diabetes. Simultaneously, elevated HbA1c levels indicate high blood sugar levels (Almugadam et al., 2021). FFAs are a type of fat found in the body that play important physiological roles, such as providing energy and contributing to the formation of cell membranes. Elevated levels of free fatty acids may be indicative of obesity or metabolic syndrome (Chen et al., 2023a). The serum levels of FIns, C-P of INS, GHbA1c and FFA were found to be significantly higher in T2DM mice compared to the NC groups, as shown in Fig. 5(E–H). After 6 weeks of intervention with TMSP1, a significant reduction in FIns, C-P of INS, GHbA1c and FFA levels was observed ($p < 0.05$). Prior research has also suggested that *Hericium erinaceus* polysaccharides can enhance insulin sensitivity, which is consistent with our current findings (Zhou et al., 2022a). These results indicated that TMSP1 could effectively enhanced insulin sensitivity in diabetic mice. Overall, these results indicated that TMSP1 exhibited the ability of hypoglycemic and repairing organ damage.

3.4. TMSP1 improved the content of liver glycogen and the liver function

In order to investigate the effect of TMSP1 on the level of glycogen

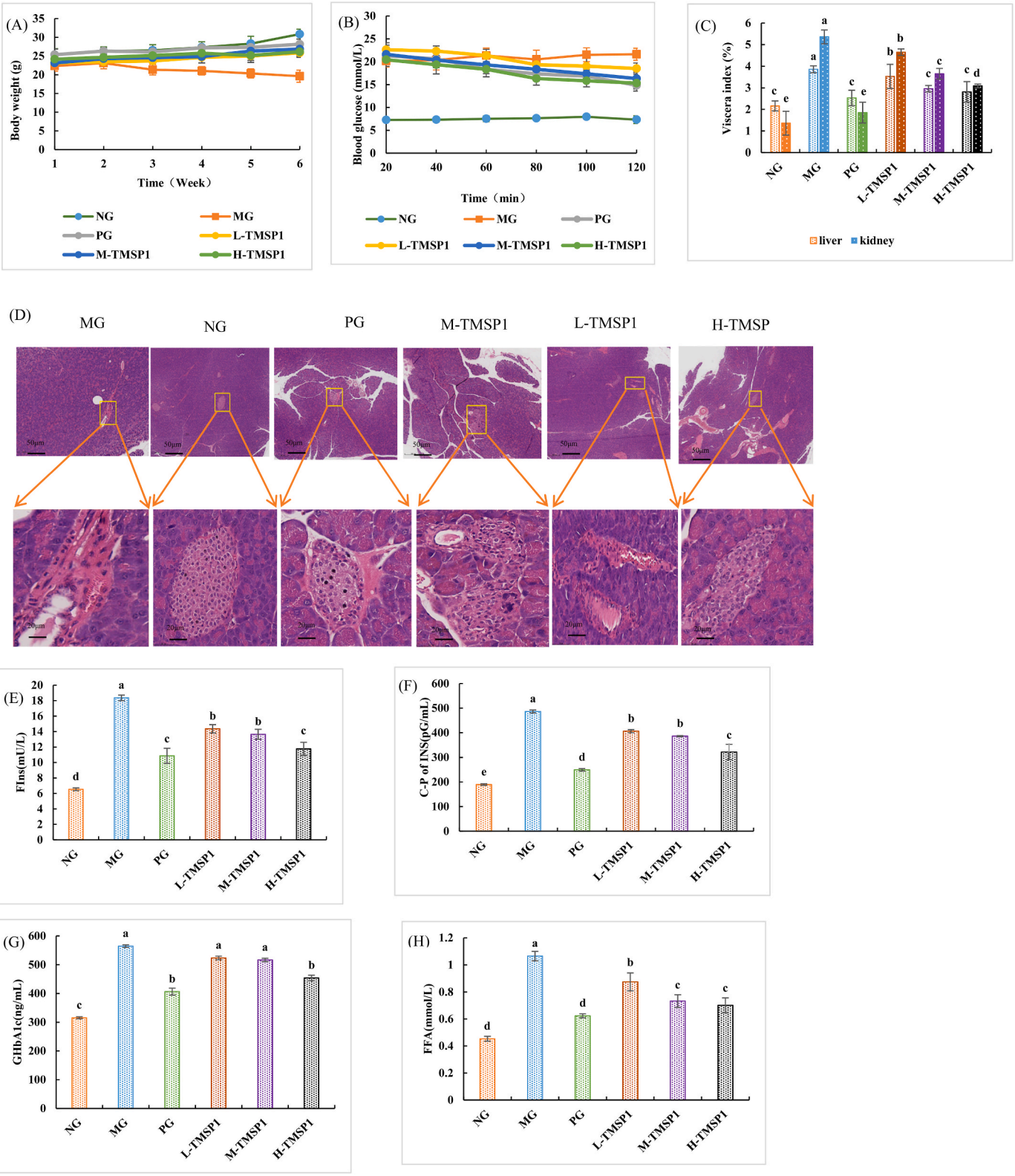

Fig. 5. Effect of TMSP1on (A) the body weight, (B) OGTT and (C) viscera index, viscera index = (organ weight/mouse weight) × 100, (D) histomorphological changes in the pancreas by H&E staining (E) FIns, (F) C-P of INS (G) GHbA1c and (H) FFA of the MG group, NG group, PG group, M-TMSP1 group, L-TMSP1 group and H-TMSP1 group, (E&H) insulin sensitivity of diabetic mice. Each group of mice was given TMSP1 for 6 weeks. Data are expressed as the means ± SEM (n = 10). Values with different letters are significantly different ($P < 0.05$). (TMSP1: *Trichosanthes kirilowii M*axim. homogeneous polysaccharide, OGTT: oral glucose tolerance test, NG: normal group, MG: mellitus control group, PG: Positive Control Group, L-TMSP1: low dose TMSP1, M-TMSP1: middle dose TMSP1, H-TMSP1: high dose TMSP1, FIns: fasting insulin, C-P of INS: insulin C-peptide, GHbA1c: Glycosylated hemoglobin A1c, FFA: Free Fatty Acids).

secretion in mice, we measured the level of serum glycogen in mice of each group. In the MG group, we observed that mice with type 2 diabetes exhibited the lowest glycogen levels, which were significantly different from those in the other groups ($P < 0.05$). This can be attributed to inadequate insulin secretion in diabetic mice, leading to impaired glycogen synthesis (Zhan et al., 2023). After 6 weeks of TMSP1 intervention, there was a significant increase in the serum glycogen content of mice. It was observed that as the polysaccharide concentration increased, there was a corresponding increase in glycogen content, indicating a clear dose-dependent effect (Fig. 6(A)). Surprisingly, no significant difference was found in serum glycogen content among the M-TMSP1, H-TMSP1 and NG groups, which indicated that TMSP1 has the potential to promote glycogen secretion. ALB is an essential protein found in human plasma, playing a vital role in regulating body nutrition and osmotic pressure. Abnormal levels of ALB may indicate irregularities in liver metabolism. AST an important indicator in liver function test, mainly exists in liver cells. The AST level may increase in the presence of necrotic liver cells, and the metabolic balance of bilirubin is crucial for liver health. Elevated TBIL levels can serve as an important indicator of liver function, suggesting potential liver injury. The levels of ALB, AST and TBIL were depicted in Fig. 6(B–D), respectively. Compared to the NG group, the MG group exhibited a significant increase in ALB, AST and TBIL levels, indicating that the high-fat and high-sugar diet combined with STZ resulted in some degree of hepatic injury in diabetic mice. After 6 weeks of polysaccharide therapy, there was a significant decrease in ALB, AST and TBIL levels ($p < 0.05$). The liver plays a crucial role in blood sugar regulation through the storage of liver glycogen, glucose metabolism, gluconeogenesis, and bile production (Lu et al., 2019). Impaired liver function can result in abnormal blood sugar metabolism, making it essential to maintain a healthy liver for normal blood sugar levels. In our study, lower levels of liver glycogen and higher levels of ALB, AST, and TBIL indicated liver damage in mice. Following TMSP1 intervention, these levels were restored, suggesting that TMSP1 could repair glycogen disorders and diabetes-induced liver damage.

3.5. TMSP1 restored enzyme activity related to blood glucose metabolism

As is commonly understood, insulin resistance often results in decreased glucose utilization and reduced expression of liver glycolytic enzymes, including HK. HK serves as the primary enzyme in glycolysis and acts as the initial rate-limiting enzyme in glucose glycogen formation (Xia et al., 2021). In Fig. 7(A), the serum HK activity was significantly lower in the DM group compared to the other groups ($P < 0.05$), indicating insulin resistance in the DM group. However, TMSP1 had a substantial effect on increasing HK activity compared to the DM group. G-6-Pase and PEPCK are two pivotal metabolic enzymes in the gluconeogenesis pathway, both of which play crucial roles in glucose metabolism (Shen et al., 2015). As shown in Fig. 7(B–C), the activities of G-6-Pase and PEPCK were remarkably elevated compared to the NC group ($P < 0.05$). However, supplementation with TMSP1 led to a significant reduction in enzyme activity. The G-6-Pase and PEPCK activities in the Met, M-TMSP1, and H-TMSP1 groups were all markedly decreased compared to the DM group ($p < 0.05$), with decrease ratios of 12.36% and 16.95%, respectively. Recent studies have demonstrated that *pumpkin* polysaccharides can mitigate hyperglycemic symptoms in mice by reducing the activity of PEPCK (Huang et al., 2023), which is in line with our findings. The findings suggested that TMSP1 may mitigate hepatocyte insulin resistance by promoting glucose metabolism within the hepatocytes.

3.6. Effect of TMSP1 on serum immune indexes

High blood sugar can have a significant impact on the immune system, leading to changes in immune indicators. Specifically, it can impair the function of immune cells and reduce defense against pathogens.

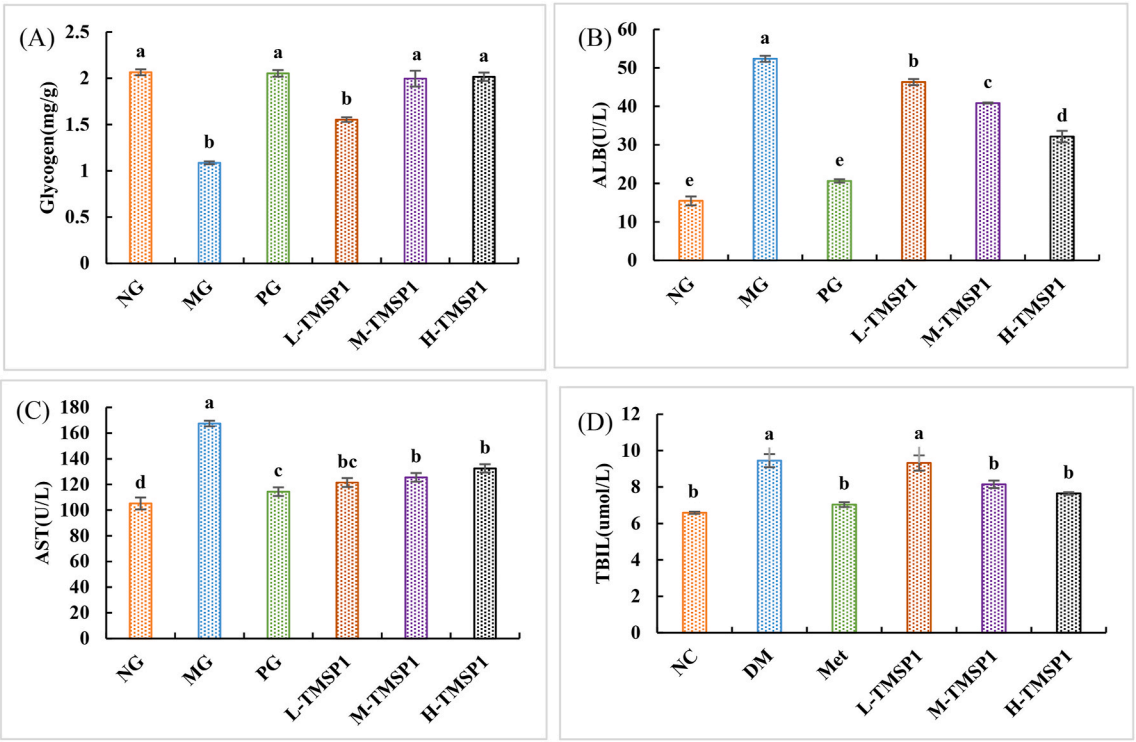

Fig. 6. TMSP1 improved the content of (A) liver glycogen and the liver function, (B) ALB, (C) AST, (D) TBIL. Each group of mice was given the corresponding dose of TMSP1 for 6 weeks. Data are expressed as the means ± SEM (n = 10). Values with different letters are significantly different ($P < 0.05$). (TMSP1: *Trichosanthes kirilowii Maxim.* homogeneous polysaccharide, ALB: albumin, AST: aspartate aminotransferase, TBIL:Total Bilirubin, NG: normal group, MG: mellitus control group, PG: Positive Control Group, L-TMSP1: low dose TMSP1, M-TMSP1: middle dose TMSP1, H-TMSP1: high dose TMSP1).

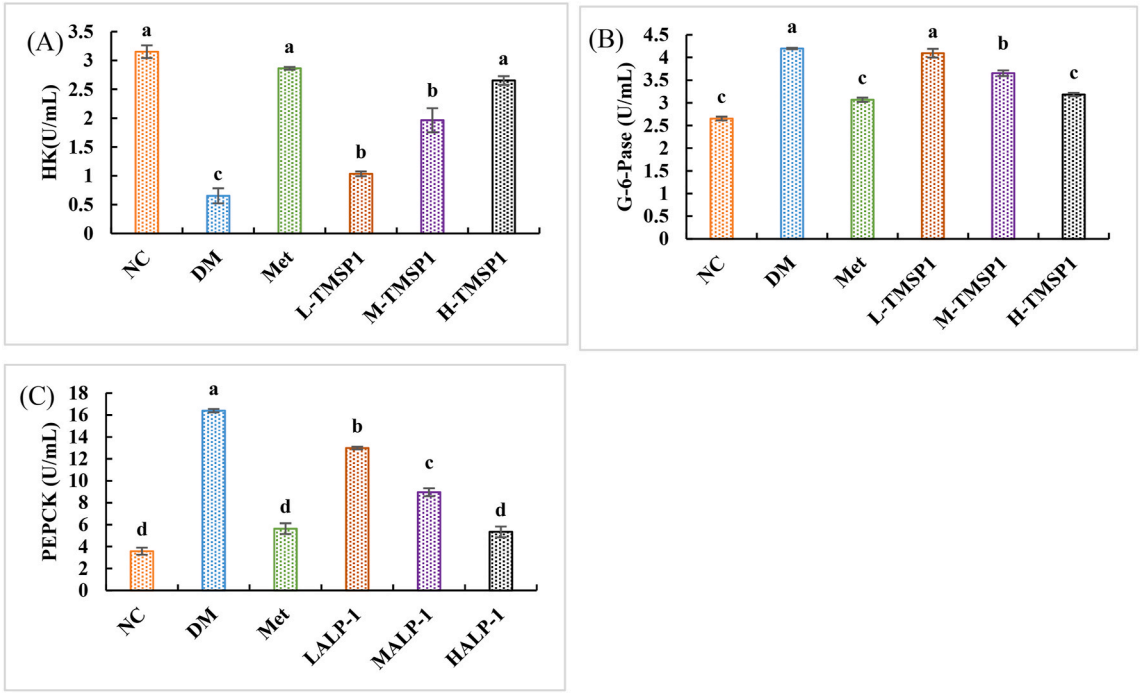

Fig. 7. Effect of TMSP1 on enzyme activity of (A) HK, (B) G-6-Pase, (C) PEPCK. Each group of mice was given the corresponding dose of TMSP1 for 6 weeks. Data are expressed as the means ± SEM (n = 10). Values with different letters are significantly different ($P < 0.05$). (TMSP1: *Trichosanthes kirilowii M*axim. homogeneous polysaccharide, NG: normal group, MG: mellitus control group, PG: Positive Control Group, L-TMSP1: low dose TMSP1, M-TMSP1: middle dose TMSP1, H-TMSP1: high dose TMSP1, PEPCK: phosphoenolpyruvate carboxykinase, HK: hexokinase, G-6-Pase: glucose-6-phosphatase).

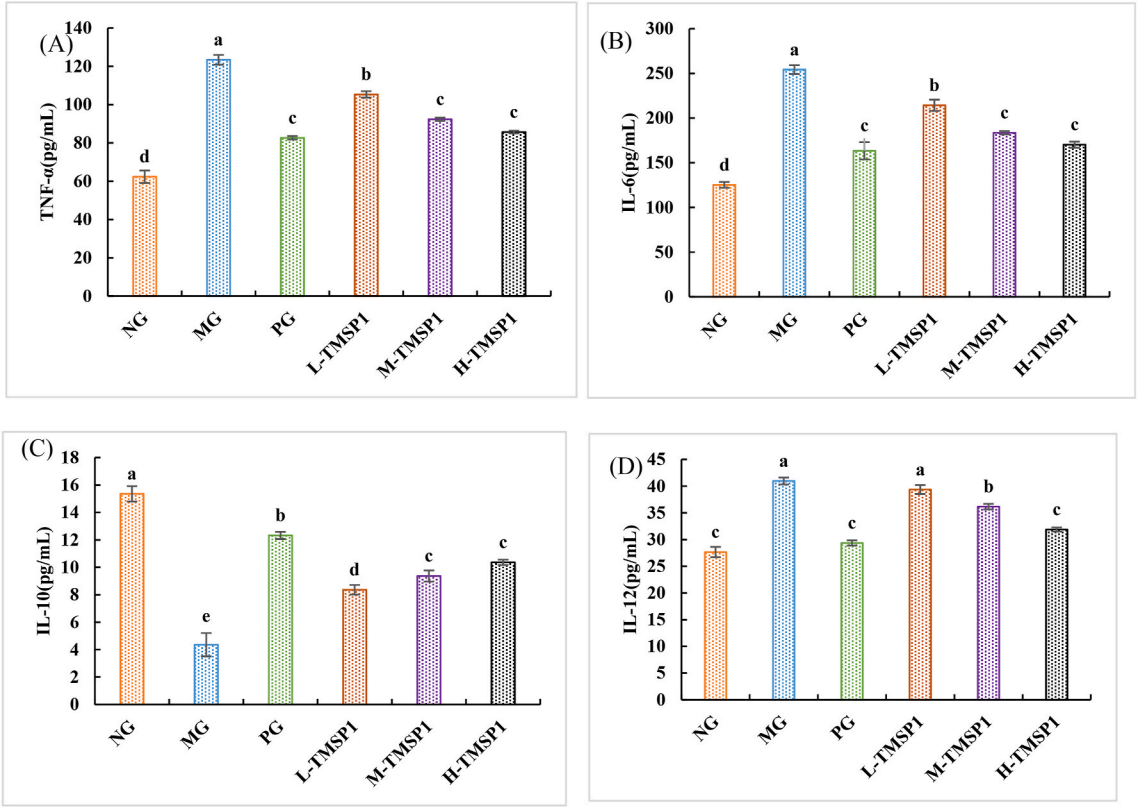

Fig. 8. Effect of TMSP1 on insulin sensitivity and serum immune indexes. (A) TNF-α, (B) IL-6, (C) IL-10, (D) IL-12. Each group of mice was given the corresponding dose of TMSP1 for 6 weeks. Data are expressed as the means ± SEM (n = 10). Values with different letters are significantly different ($P < 0.05$). (TMSP1: *Trichosanthes kirilowii M*axim. homogeneous polysaccharide, NG: normal group, MG: mellitus control group, PG: Positive Control Group, L-TMSP1: low dose TMSP1, M-TMSP1: middle dose TMSP1, H-TMSP1: high dose TMSP1, TNF-α: Tumor Necrosis Factor-α, IL-6: Interleukin-6, IL-10: Interleukin-10, and IL-12: Interleukin-12).

Additionally, it can result in abnormal levels of immune factors, characterized by increased TNF-α, IL-6 and IL-12, as well as decreased IL-10 (Fan et al., 2017b). As shown in Fig. 8(A–D), the serum levels of TNF-α, IL-6 and IL-12 were significantly elevated in mice from the MG group, while the level of IL-10 expression was notably reduced compared to the NG group ($p < 0.05$). As expected, supplementation with TMSP1 effectively suppressed the changes in TNF-α, IL-6, IL-12 and IL-10 expression levels ($p < 0.05$). Similarly to a previous study, *Phyllanthus emblica* polysaccharide also improved blood sugar levels by restoring the expression of inflammatory factor (Habib et al., 2017). A recent study showed that *Momordica charantia* polysaccharide has the potential to protect against early-stage diabetic by modulating cytokines (Liu et al., 2023). In another study, polysaccharide from *Inonotus obliquus* could reduced serum TNF-α and IL-6 levels to exhibit hypoglycaemic effects (Su et al., 2022). These findings were consistent with present result. In conclusion, the TMSP1 intervention demonstrated the potential to restore immune response in mice with type 2 diabetes.

3.7. TMSP1 increased the contents of SCFAs of intestinal contents

SCFAs are primarily produced through the anaerobic metabolism of bacteria in the colon, with fermentation by intestinal flora resulting in the production of acetic acid, propionic acid, butyric acid, and other carbohydrates. They are not only important organic acid anions in the colon, but also an important source of energy (Chen et al., 2020c). Alterations in the SCFAs and the total content were shown in Fig. 9(A–I). Compared with NG group, the contents of acetic acid, propionic acid, butyric acid, isobutyric acid, valerate acid, isovalerate acid, hexanoic acid, isohexanoic acid and total SCFAs in MG group were significant decreased ($p < 0.05$). After the TMSP1 intervention, there was a significant increase in the levels of these SCFAs, demonstrating a notable elevation compared to the MG group ($p < 0.05$). Previous research has suggested that SCFAs can positively impact the maintenance of blood glucose balance (Qu et al., 2018). Acetic acid, as a short-chain fatty acid, can enhance glucose homeostasis by promoting insulin secretion and sensitivity, showing potential for adjunctive treatment of type 2

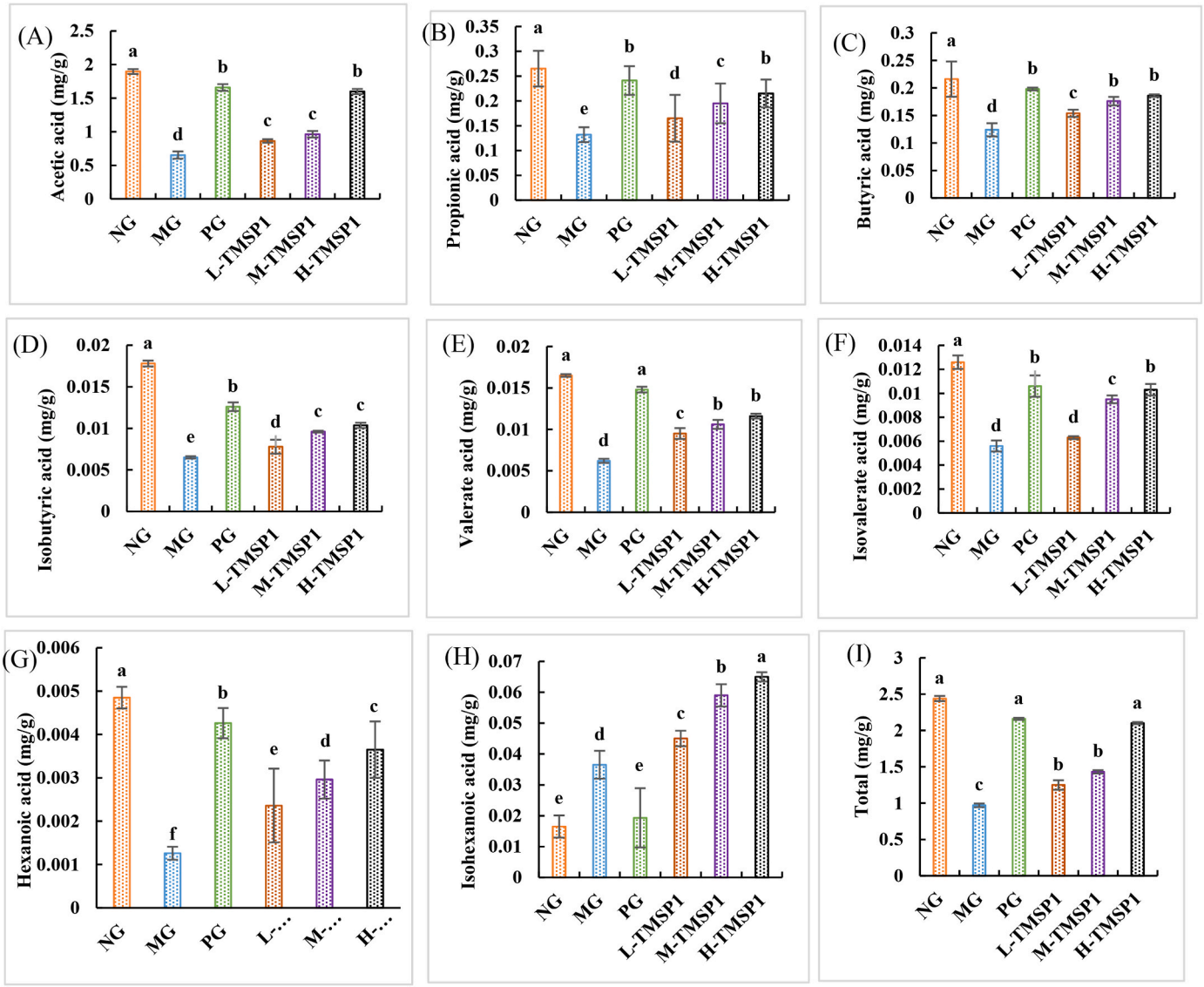

Fig. 9. The effect of TMSP1 on the content of SCFAs in the cecum of T2DM rats. (A) Acetic acid, (B) Propionic acid, (C) Butyric acid, (D) Isobutyric acid, (E) Valerate acid, (F) Isovalerate acid, (G) Hexanoic acid, (H) Isohexanoic acid, (I) Total. Each group of mice was given the corresponding dose of TMSP1 for 6 weeks. Data are expressed as the means ± SEM (n = 10). Values with different letters are significantly different ($P < 0.05$). (TMSP1: *Trichosanthes kirilowii Maxim.* homogeneous polysaccharide, NG: normal group, MG: mellitus control group, PG: Positive Control Group, L-TMSP1: low dose TMSP1, M-TMSP1: middle dose TMSP1, H-TMSP1: high dose TMSP1).

diabetes. Propionic acid and butyric acid stimulate gluconeogenesis in the gut, converting non-sugar compounds into glucose or glycogen to improve insulin sensitivity throughout the body. Meanwhile, isovalerate acid may impact blood sugar levels through regulation of the gut microbiome (Chen et al., 2021). Liu and his colleagues found that polysaccharides from *Phellinus linteus* could promote SCFAs production to attenuate type 2 diabetes mellitus (Liu et al., 2024). Moreover, previous publication had reported that *Ascophyllum nodosum* polysaccharides had the capacity of hpyerglycemic by increasing the contents of acetate acid, propionate acid and butyric acid in mice (Chen et al., 2023b), which was also consistent with our results. In summary, TMSP1 supplementation altered type 2 diabetes by alleviating various short-chain fatty acid disorders and increasing the total amount of SCFAs.

3.8. Oxidative stress analysis

Recent studies have established a robust correlation between oxidative stress and diabetes, along with its long-term complications (Cardullo et al., 2020b). MDA, SOD, and GSH-Px are commonly utilized as important reference indicators for assessing oxidative stress damage. SOD functions to eliminate superoxide anion free radicals, thereby maintaining the body's oxidation and antioxidant balance and protecting cells from damage. GSH-Px is an enzyme responsible for breaking down peroxides in the body, specifically catalyzing the reduction of reduced glutathione to hydroperoxide and protecting the structural and functional integrity of cell membranes. MDA serves as a representative thiobarbituric acid reactant, used as a marker for measuring lipid peroxide levels (Wang et al., 2019). In Fig. 10(A–C), the H-TMSP1 group demonstrated a significant increase of 9.35% in GSH-Px activity and a remarkable increase of 216.35% in SOD activity compared to the MG group, while the MDA content decreased significantly by 62.76%. Meanwhile, the results indicated that there was no significant difference in the activities of GSH-Px and SOD, as well as MDA content, between the H-TMSP1 group and PG group. It was speculated that TMSP1 could improve the effect of scavenging free radicals by regulating the level of relevant enzymes.

3.9. Histopathological analysis

The histopathological examination of the kidney in Fig. 11 demonstrates normal renal architecture in the NG group, characterized by clear glomeruli and renal tubules, with no evidence of inflammatory infiltration or urate crystals (Fig. 11(A)). The MG group exhibited atrophic glomeruli, dilated renal tubules, and uric acid crystals in the lumen compared to the NG group. Additionally, there was obvious swelling and necrosis of the epithelial cells of renal tubules, vacuolar degeneration, appearance of uric acid crystals in the pericyma, and inflammatory cell infiltration in the renal interstitium (Fig. 11B). The PG group exhibited no significant glomerular atrophy and reduced dilation of the renal tubule lumen compared to the MG group (Fig. 11F). After 4 weeks of polysaccharide administration, the renal tissue in each group showed improvement, with glomeruli approaching normal structure, shape and size. The wall and lumen size of proximal and distal tubules also improved, reducing swelling, although some areas still exhibited a small amount of inflammatory cell infiltration (Fig. 11C–E). In addition, the renal tubule injury score showed that the intervention of TMSP1 significantly inhibited the renal tubule injury in mice, and the inhibitory effect was enhanced with the increase of dose (Fig. 11 G).

The histopathological examination of the liver was depicted in Fig. 12. Under normal physiological conditions, the H&E staining of liver tissue revealed a well-organized and regular hepatic architecture. Furthermore, the cells exhibited distinct boundaries, compact and uniform arrangement, with no evidence of cellular degeneration or abnormalities (Fig. 12 A). The hepatic cells of the MG group exhibited disorganization, with cytoplasm containing fat vacuoles of varying sizes and a significant area occupied by fat droplets, accompanied by mild inflammation (Fig. 12 B). Compared to the MG group, the L-TMSP1 and M-TMSP1 groups showed a reduction in both the volume and number of fat vacuoles in the liver, leading to a certain degree of inhibition of steatosis (Fig. 12C–D). However, the L-TMSP1 group still exhibited significant fat vacuoles. The liver lipid accumulation of mice in the PC and H-TMSP1 groups showed significant improvement, with tissue structure approaching normal despite some minor inflammation (Fig. 12E–F). Based on the histopathology results, it can be concluded that TMSP1 exhibited a specific reparative effect on kidney and liver damage in T2DM mice, which was consistent with the decreased histological injury score (Fig. 12 G).

3.10. TMSP1 mitigated colon histomorphology and promoted ZO-1, occludin expression in T2DM mice

Additionally, we postulated that the impact of TMSP1 on alleviating hyperglycemia symptoms may be closely associated with the reinforcement of the intestinal barrier. As shown in Fig. 13(A), in the NG group, the colonic villi were arranged closely and neatly, with a moderate intestinal wall thickness and no apparent injury. In the MG group, villi exhibited disorganization and swelling, the intestinal wall showed vacuolation and necrosis, and there was increased infiltration of inflammatory cells. Following polysaccharide intervention, the damage to intestinal tissue and villus lesions in mice were alleviated to varying degrees, leading to improved tissue integrity.

The presence of transmembrane proteins is essential for maintaining the integrity of the intestinal barrier, thereby preventing harmful substances such as endotoxins and pathogens from entering the bloodstream (Chen et al., 2021). The immunofluorescence method was utilized to evaluate the expression of ZO-1 and occludin in colon tissues (Fig. 13B–D), revealing a significant reduction in their expression in the

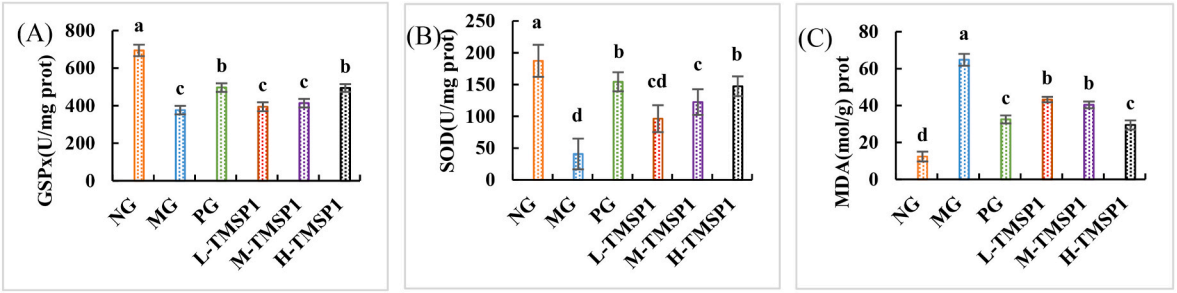

Fig. 10. Effects of TMSP1 on activities of SOD and GSH-Px and the concentrations of MDA. (A) GSH-Px, (B) SOD, (C) MDA. Each group of mice was given the corresponding dose of TMSP1 for 6 weeks. Data are expressed as the means ± SEM (n = 10). Values with different letters are significantly different ($P < 0.05$). (TMSP1: *Trichosanthes kirilowii M*axim. homogeneous polysaccharide, NG: normal group, MG: mellitus control group, PG: Positive Control Group, L-TMSP1: low dose TMSP1, M-TMSP1: middle dose TMSP1, H-TMSP1: high dose TMSP1, GSPx: glutathione peroxidase, SOD: superoxide dismutase, MDA:malondialdehyde).

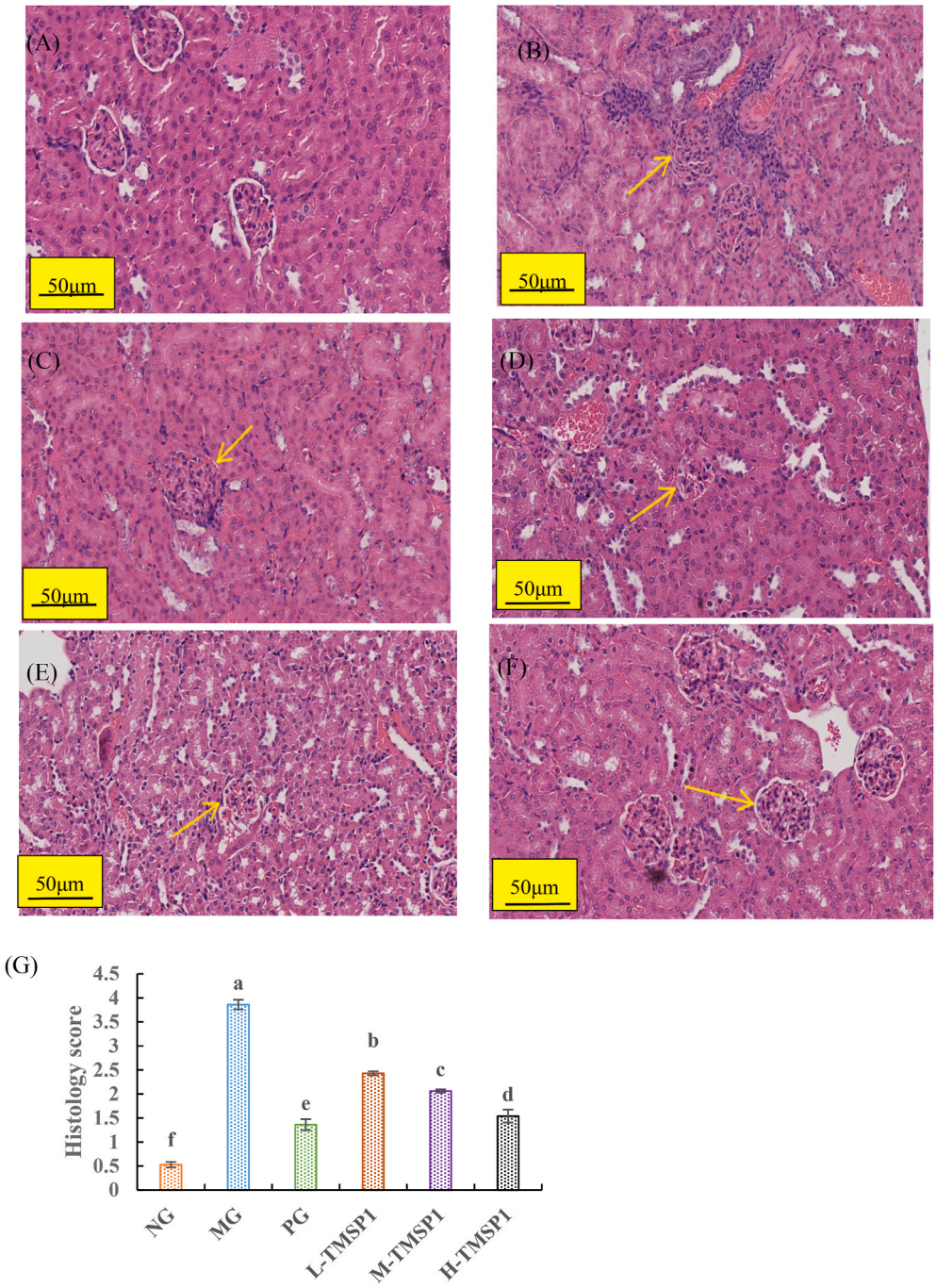

Fig. 11. Pathological changes of kidney, and scale bar = 50 μm. (A) NG group, (B) MG group, (C) L-TMSP1 group, (D) M-TMSP1 group, (E) H-TMSP1 group, (F) PG group, (G) The renal pathology score of each group. Each group of mice was given the corresponding dose of TMSP1 for 6 weeks. (TMSP1: *Trichosanthes kirilowii Maxim.* homogeneous polysaccharide, NG: normal group, MG: mellitus control group, PG: Positive Control Group, L-TMSP1: low dose TMSP1, M-TMSP1: middle dose TMSP1, H-TMSP1: high dose TMSP1).

MG group. After the administration of polysaccharides, particularly in the M-THSP1 and H-TMSP1 groups, there was a significant restoration of the STZ-induced decrease in ZO-1 and occludin expression. This suggests that supplementation with polysaccharides may enhance the expression of tight junction proteins to protect against damage to the intestinal mechanical barrier caused by disease. Therefore, *Trichosanthes kirilowii* Maxim. polysaccharide could improve the intestinal barrier function of diabetic mice.

3.11. Intestinal microbiota analysis

The results of the OTU cluster analysis using the optimized clean tags are depicted in Fig. 14(A). It is evident from the figure that there were 74 unique OTUs in the NC group, 28 OTUs in the MG group, and 23 OTUs in the H-TMSP1 group. The dilution curve and Shannon-Winner curve are primarily indicative of the sequencing depth and microbial diversity in the samples. As random sequencing increases, more OTUs are discovered, causing the dilution curve to rise before reaching a plateau, indicating that the amount of sequencing data was appropriate (Fig. 14 B). Shannon-Winner curve (Fig. 14 C) continued to rise and reached a

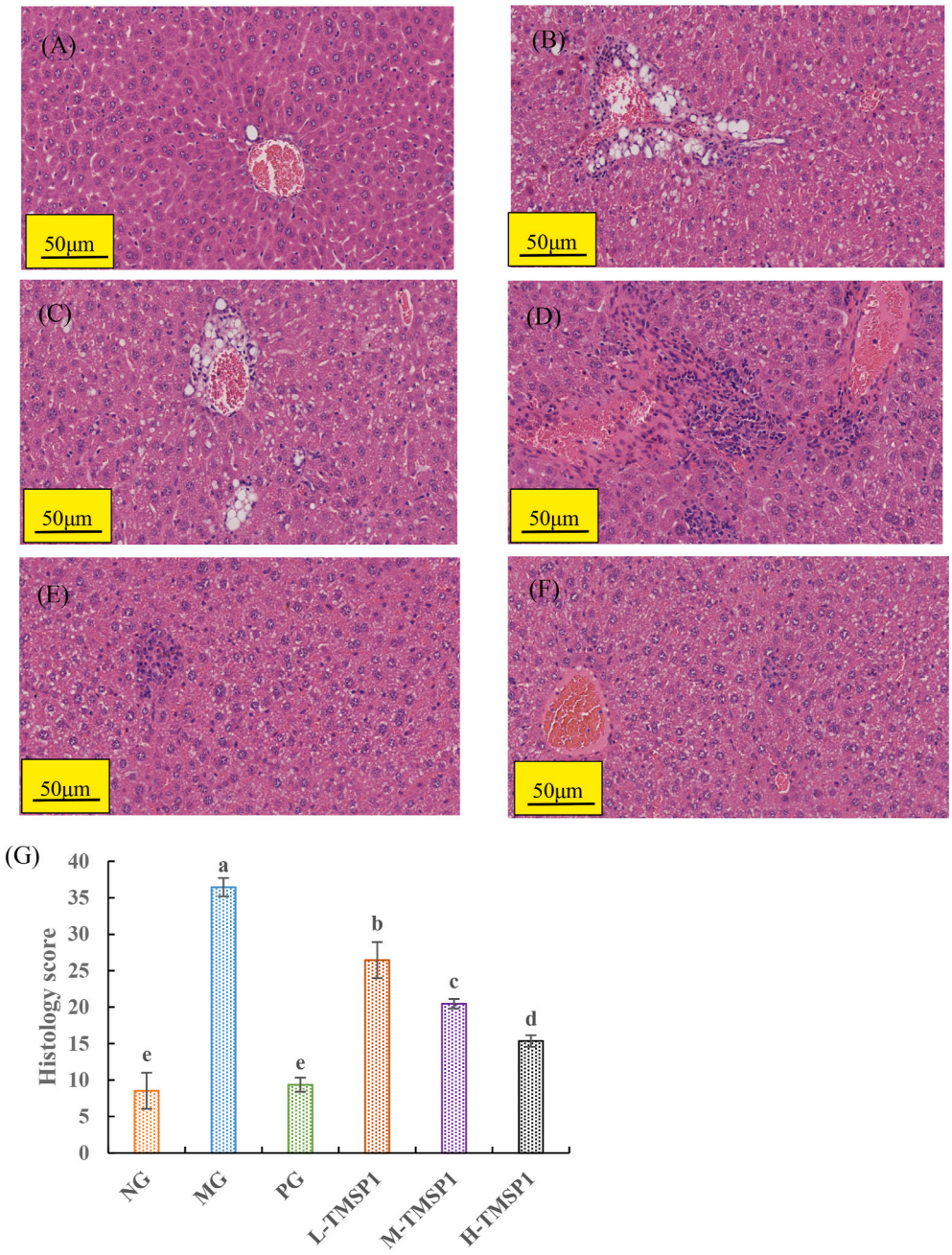

Fig. 12. Pathological changes of liver, and scale bar = 50 μm. (A) NG group, (B) MG group, (C) L-TMSP1 group, (D) M-TMSP1 group, (E) H-TMSP1 group, (F) PG group, (G) Calculated histological scores. Each group of mice was given the corresponding dose of TMSP1 for 6 weeks. (TMSP1: *Trichosanthes kirilowii M*axim. homogeneous polysaccharide, NG: normal group, MG: mellitus control group, PG: Positive Control Group, L-TMSP1: low dose TMSP1, M-TMSP1: middle dose TMSP1, H-TMSP1: high dose TMSP1).

plateau, indicating that the sequencing data is adequate for capturing the complete diversity of bacterial flora (Wu et al., 2021). The α diversity index reflects the richness and diversity of the microbial community. Moreover, Shannon index reflects microbial richness, while the Simpson index and Chao1 index primarily reflect microbial diversity (Lunken et al., 2021). The Shannon index of intestinal flora in mice from the MG group, as shown in Fig. 14(D), exhibited the highest level, indicating a significant difference compared to both the NG group and H-TMSP1 group ($P < 0.05$). This suggests a notable increase in the abundance of flora in type 2 diabetes mice induced by a high-fat diet and STZ. After 6 weeks of TMSP1 intervention, the abundance of intestinal flora in diabetic mice decreased significantly, indicating that TMSP1 could alleviate the disorder of intestinal flora in mice to a certain extent. The Simpson index and Chao1 index of intestinal flora in the MG group exhibited the highest values, indicating a significant increase in microbial diversity. Following 6 weeks of polysaccharide treatment, there was a notable decrease in the diversity of intestinal flora in diabetic mice. β diversity analysis primarily served to illustrate the similarity of intestinal flora composition among different samples (Wang et al., 2022b). Principal co-ordinates analysis (PCoA) reflects the similarity or difference of sample community composition (Wu et al., 2022c). Fig. 14(F) clearly demonstrates a distinct separation in the PC2 ordinate dimension, with the MG group being significantly different from both the NG group and H-TMSP1 group, indicating significant differences in community composition between the MG group and the other groups, while showing minimal distinctions between the NG group and H-TMSP1

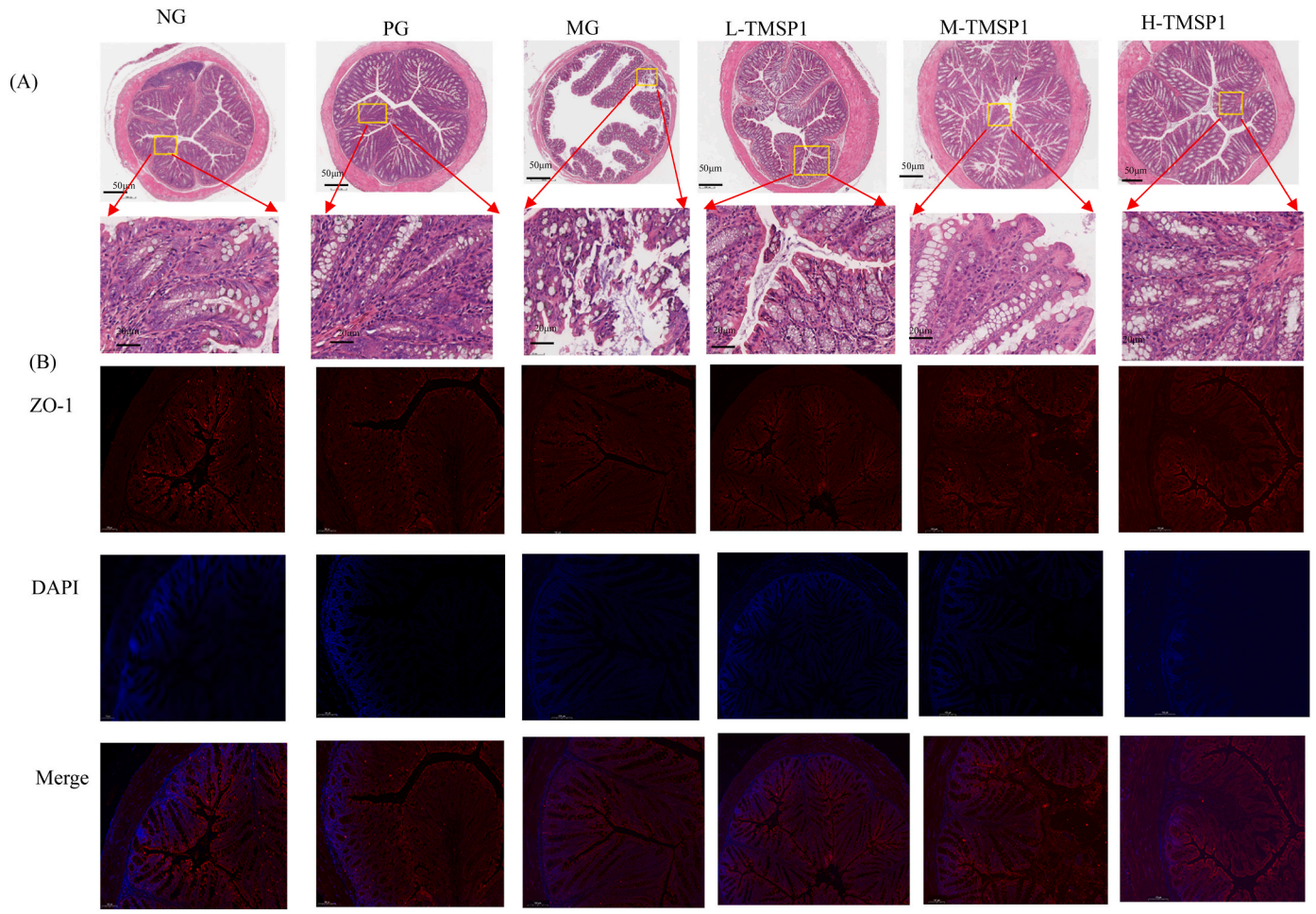

Fig. 13. (A) Histopathological staining in colon, (B–C) Representative fluorescent images of Occludin and ZO-1 in colon tissues, (D) The fluorescence intensity of Occludin and ZO-1. Data are expressed as the means ± SEM (n = 10). Each group of mice was given the corresponding dose of TMSP1 for 6 weeks. Values with different letters are significantly different ($P < 0.05$). (TMSP1: *Trichosanthes kirilowii M*axim. homogeneous polysaccharide, NG: normal group, MG: mellitus control group, PG: Positive Control Group, L-TMSP1: low dose TMSP1, M-TMSP1: middle dose TMSP1, H-TMSP1: high dose TMSP1, ZO-1: zonulaoccluden-1, DAPI: 4′,6-Diamidino-2-phenylindole).

group. Fig. 14(E) showed that the MG group was separated from the other groups. However, the NG group and H-TMSP1 group distributed in the same region of the two-dimensional planar graph composed of PC1 and PC2. The results showed that the intestinal flora structure of mice in H-TMSP1 group was significantly changed compared with that in MG group.

To identify the specific bacterial groups within the intestinal microbiota of each group, a linear discriminant analysis (LDA) threshold of 3 was set. Additionally, the linear discriminant analysis effect size (LEfSe) was utilized to analyze differences at all classification levels in the intestinal microbiota of mice (Duan et al., 2022). As can be seen from Fig. 15(A–B), more dominant flora appeared in NG group at different classification levels. At the order level, Burkholderiales, Oceanospirillales, Aeromonadales and Sphingobacteriales were the dominant microflora of NG group mice. At the phylum level, Proteobacteria was the dominant microflora. Moreover, at the family level, Alcaligenaceae, Halomonadaceae, Aeromonadaceae, Sphingobacteriaceae and Pseudomanad were the dominant microflora. At the genus level, Halomonas, Erysipelothrix, Oceanisphaera and Pseudomonas were the dominant microflora. in addition, Rhodospirillales, Hungateiclostridiaceae and Clostridia were the dominant microflora in H-TMSP1 group. However, only Marinifilaceae was the dominant bacterial in MG group. Bacterial abundance was measured at different taxon levels to confirm the changes of intestinal microbial structure induced by TMSP1 intervention. As shown in Fig. 15(C), all groups had five dominant phyla (Firmicutes, Bacteroidota, Deferribacterota, Desulfobacterota, Desulfobacterota and Campilobacterota). Firmicutes was higher in MG group than that in NG group, Bacteroidota was lower in NG group, and supplementation with TMSP1 reversed these changes. Previous study has shown that their ratio (Firmicutes/Bacteroidota F/B) was related to intestinal absorption capacity (Ribovski et al., 2021). F/B in MG group was the highest, and the absorption capacity of MG group mice was the best. NG group and H-TMSP1 group had low F/B and weak nutrient absorption ability, which helped to reduce the blood sugar level of mice. The abundance of Deferribacterota and Desulfobacterota in MG group were higher than those in NG group and H-TMSP1 groups. After 6 weeks of TMSP1 intervention, the abundance of these two phyla decreased in mice. It has been reported that hydrogen sulfide is the main product of Deferribacterota and Desulfobacterota. High concentration of hydrogen sulfide may destroy intestinal cells due to its toxicity, and is genotoxic and cytotoxic to animal cells. The generic level composition of bacterial types is shown in Fig. 15(D), *Muribaculaceae*, *Mucispirillum*, *Lachnospiraceae_NK4A136_group*, *Helicobacter* and *Alistipes* account for the majority of the total species at the genus level, and belonging to the dominant flora at the genus level. The MG group had a higher *Muribaculaceae* abundance and a lower *Mucispirillum* abundance than the NG group. After polysaccharide intervention, the abundance of beneficial bacteria *Mucispirillum*, *Lachnospiraceae* and *Alistipes* were increased. Previous studies have shown that *Mucispirillum* is a dominant bacterial group in the intestinal tract of mice, which can metabolize and produce SCFAs

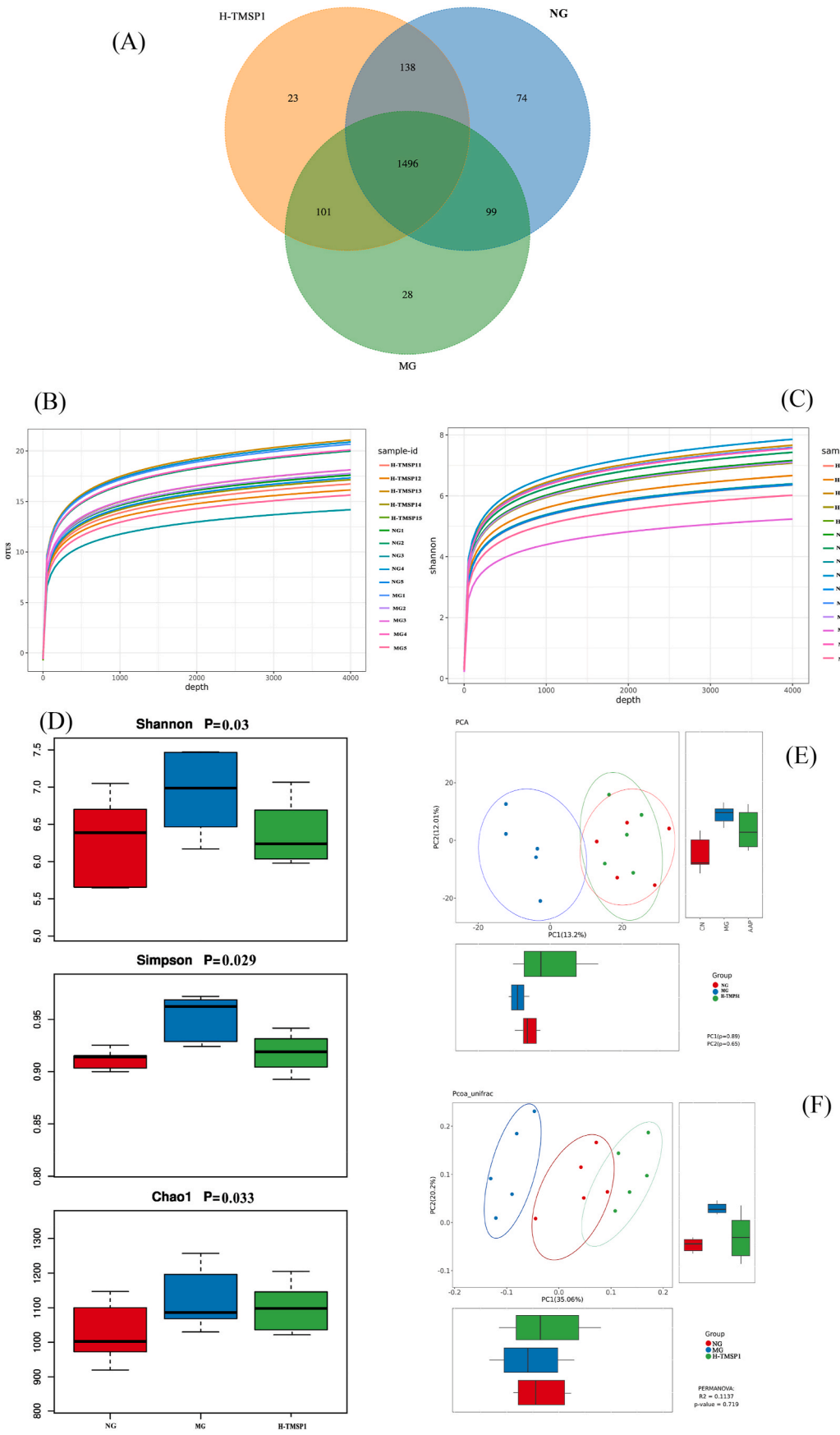

Fig. 14. (A) Venn diagram of the OTUs number in each group,(B) Rarefaction Curve, (C) Shannon-Winner Curve, (D) α diversity analysis, (E) β diversity analysis. Each group of mice was given the corresponding dose of TMSP1 for 6 weeks. (TMSP1: *Trichosanthes kirilowii M*axim. homogeneous polysaccharide, NG: normal group, MG: mellitus control group, H-TMSP1: high dose TMSP1).

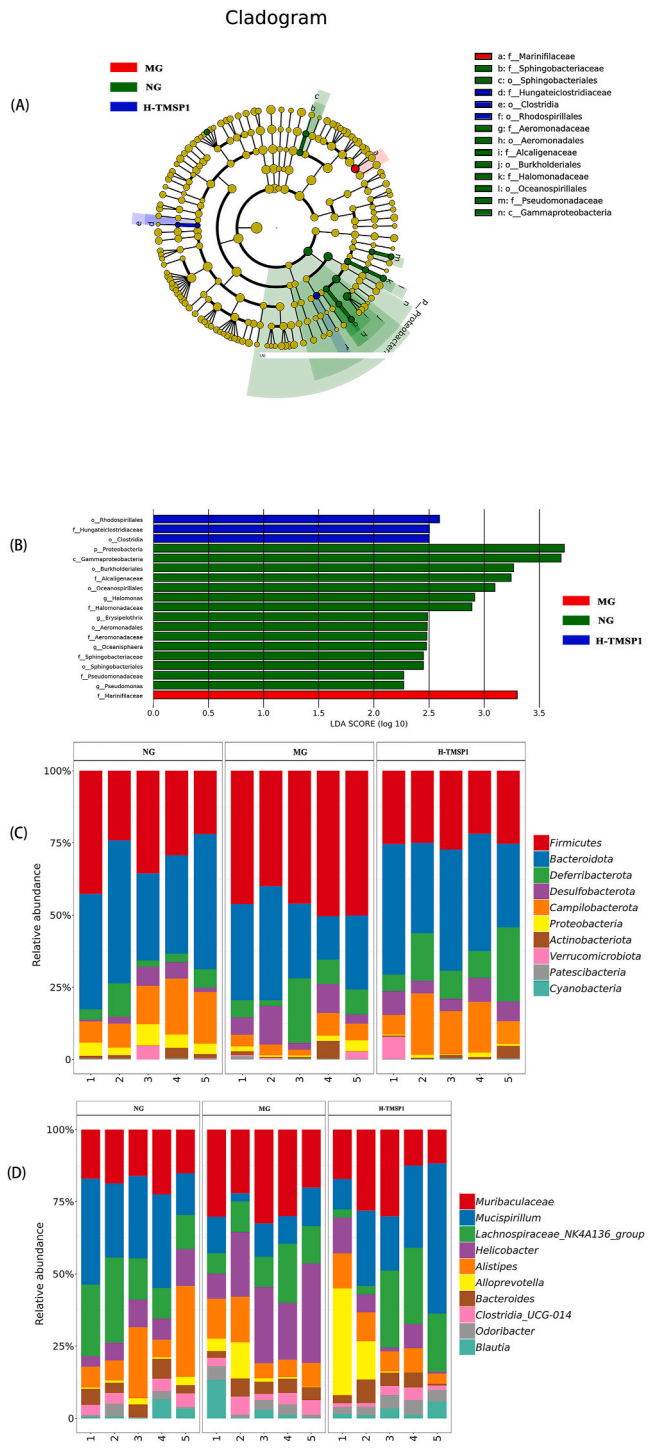

Fig. 15. (A) Branch diagram visualizes LEfSe analysis results, (B) The most significant difference in intestinal microbiota was found among the groups after LDA, (C–D) compositional changes of gut microbes at the phylum/genus level. Each group of mice was given the corresponding dose of TMSP1 for 6 weeks. (TMSP1: *Trichosanthes kirilowii M*axim. homogeneous polysaccharide, NG: normal group, MG: mellitus control group, H-TMSP1: high dose TMSP1, H-TMSP1-FMT: microflora of H-TMSP1 group was injected into recipient mice, MG-FMT: microflora of MG group was injected into recipient mice).

(Zhang et al., 2020b). In addition, *Lachnospiraceae*, an important producer of SCFAs, is able to provide energy and selectively up-regulate the expression of tight junction proteins, which can promote the integrity of intestinal epithelium (Yi et al., 2020). *Alistipes* is considered to be a genus of intestinal bacteria that can regulate metabolism, improve intestinal immunity, and promote the body's resistance to diseases (Cheng et al., 2020). Therefore, the fermentation of TMSP1 can increase the beneficial microorganisms and reduce the relative abundance of helicogenic bacteria, and regulate the structure of intestinal flora and improve intestinal health.

The functional prediction analysis of intestinal bacteria in mice in each group was shown in Fig. 16. The enriched KEGG pathways were screened, and the pathways with an average value $< 0.01\%$ were excluded and 9 KEGG Level pathways were mainly enriched. Function prediction at level 3 based on KEGG is shown the intestinal flora of MG group and H-TMSP1 group were significantly different in terms of Typtophan metabolism, Chlorocyclohexane and chlorobenzene degradation, Secondary bile acid biosynthesis, Primary bile acid biosynthesis, Chloroalkane and chloroalkene degradation, Ascorbate and aldarate metabolism, Caprolactam degradation, Phosphotransferase system and Protein processing in endplasmic reticulum ($P < 0.05$). By comparison, it was found that after polysaccharide intervention 6, the metabolism of Typtophan in the intestinal flora of mice was enhanced. At the same time, the degradation pathways of Chlorocyclohexane, chlorobenzene, Chloroalkane, Caprolactam and chloroalkene also increased. in addition, the intervention of polysaccharide also had promoting effect on Phosphotransferase system and Protein processing.

In order to explore the changes of functional genes of mouse intestinal flora in metabolic pathways, STAMP difference analysis was performed on the intestinal flora of mice in each group (Sanna et al., 2019). As can be seen from Fig. 17(A), STZ could change the functional abundance of 18 mice intestinal flora, among which 6 functional abundance was increased and 12 functional abundance was decreased. Increased feature abundance was primarily related to transport and metabolism, cell community, signal transduction, synthesis of secondary metabolites, environmental adaptation and endocrine and metabolic diseases. In addition, the reduced functional abundance is mainly related to signaling molecules and interactions, nervous system, membrane transport, nucleotide metabolism, lipid metabolism, and so on, which indicated that STZ induced changes the metabolic capacity of intestinal flora in mice. 6 weeks after polysaccharide intervention, the functional abundance of intestinal flora in mice also changed, with a total of 11 functional abundance changes: 7 functional abundance was significantly increased, and 4 functional abundance was significantly decreased. This involves metabolic systems such as amino acid metabolism, transport and catabolism, lipid metabolism and synthesis of secondary metabolites, as well as major diseases such as endocrine and metabolic diseases, immunological diseases (Fig. 17(B)). It can be concluded that after metabolism of TMSP1 in mice, the type and abundance of intestinal flora was changed, so as to regulating the hypoglycemic ability of mice.

3.12. Serum biochemical detection of recipient mice after FMT experiment

With the development of intestinal microbiology, fecal microbiome transplantation technology has attracted more and more attention. FTM is a kind of technical means to reconstruct intestinal microecosystem by transplanting intestinal microbes from healthy donors into the intestines of diseased recipients. As shown in Fig. 18(A), compared with the body mass of mice in the MG-FMT group, the body weight of mice in the H-TMSP1-FMT group increased significantly from 0 to 8 weeks of the experiment, with statistical significance ($P < 0.05$). The results of OGTT experiment showed that compared with MG-FMT group, the area under OGTT curve of mice in MG-FMT group showed a decreasing trend (Fig. 18(B)). The blood glucose of the recipient mice decreased by 20.81% after transplanting the intestinal microbes of the donor mice with *Trichosanthes kirilowii* Maxim polysaccharide. Zhou's research showed that after receiving *Lycium barbarum* polysaccharide through fecal bacteria transplantation, the blood sugar of the recipient mice decreased by 16.34% (Zhou et al., 2022b). At the same time, the result of FINS and TBIL concentrations revealed that compared with MG-FMT

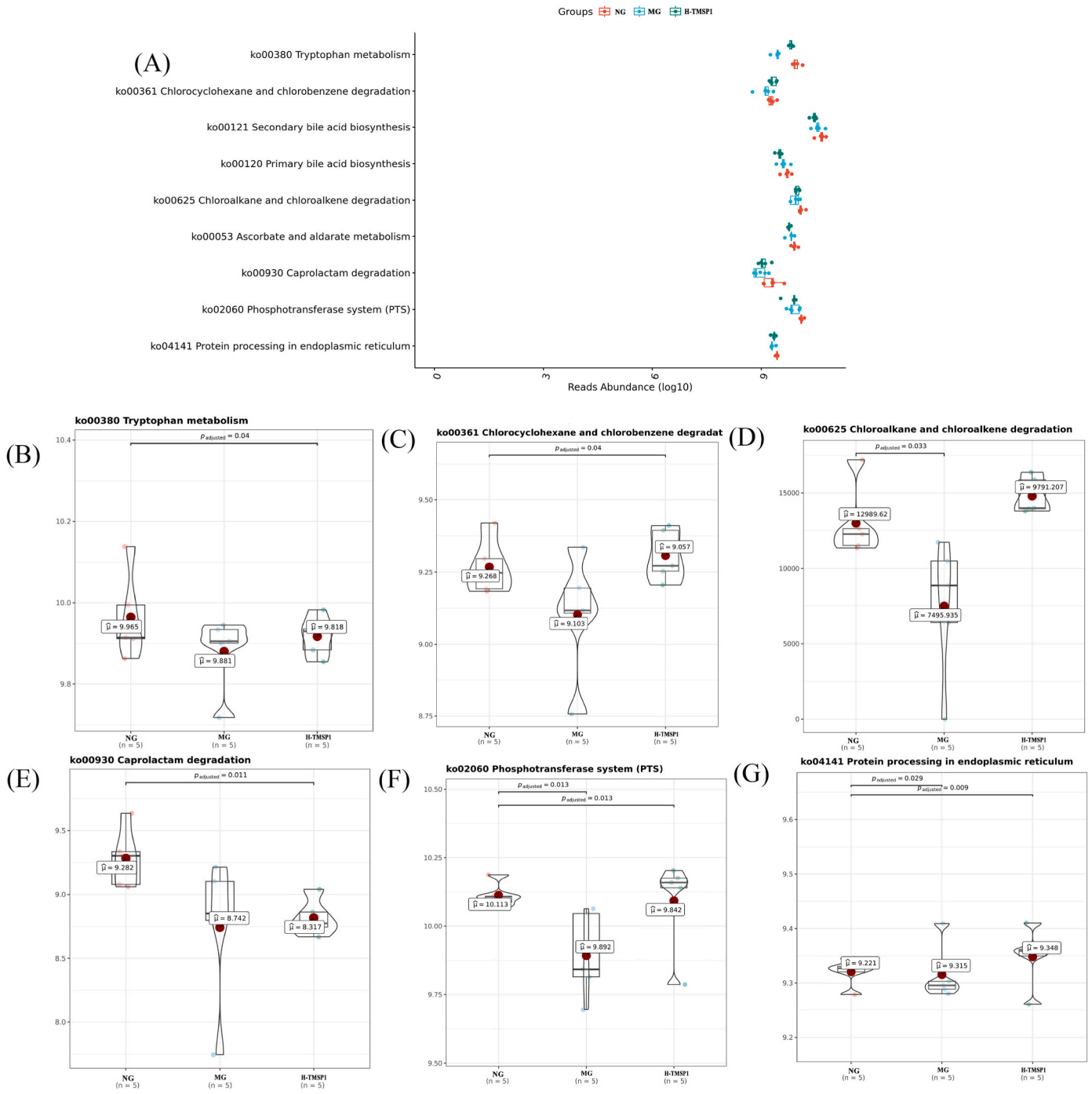

Fig. 16. (A) Predictive functional profiling of microbial communities by PICRUSt. (B) Comparison of tryptophan metabolism of each group, (C) Comparison of chlorocyclohexane and chlorobenzene degradat of each group, (D) Comparison of chloroalkane and chloroalkene degradation of each group, (E) Comparison of Caprolactam degradation of each group, (F) Comparison of Phosphotransferase system (PTs) of each group, (G) Comparison of Protein processing in endoplasmic reticulum of each group. Each group of mice was given the corresponding dose of TMSP1 for 6 weeks. (TMSP1: *Trichosanthes kirilowii Maxim.* homogeneous polysaccharide, NG: normal group, MG: mellitus control group, H-TMSP1: high dose TMSP1).

group, the FINS and TBIL concentrations in H-TMSP1-FMT group were significantly decreased ($P < 0.05$) (Fig. 18(C)). However, the result of glycogen concentrations showed an obviously opposite trend (Fig. 18 (D)). In addition, the AUC of blood glucose curves in H-TMSP1-FMT group (1625.4 mmol/L·min) decreased by 9.90% compared with MG-FMT group (1803.8 mmol/L·min), which was consistent with the above results. These results suggested that TMSP1 could restore the intestinal microbial structure of type 2 diabetic mice, and effectively inhibit the disorder of glucose and lipid metabolism of high-fat diet mice through FTM.

4. Conclusion

In conclusion, we purified a homogeneous polysaccharide (TMSP1) from *Trichosanthes kirilowii* Maxim, and further confirmed the hypoglycemic effects of TMSP1. At the same time, the changes of intestinal flora composition and function after TMSP1 treatment were revealed. Our results showed that TMSP1 intervention decreased lipid

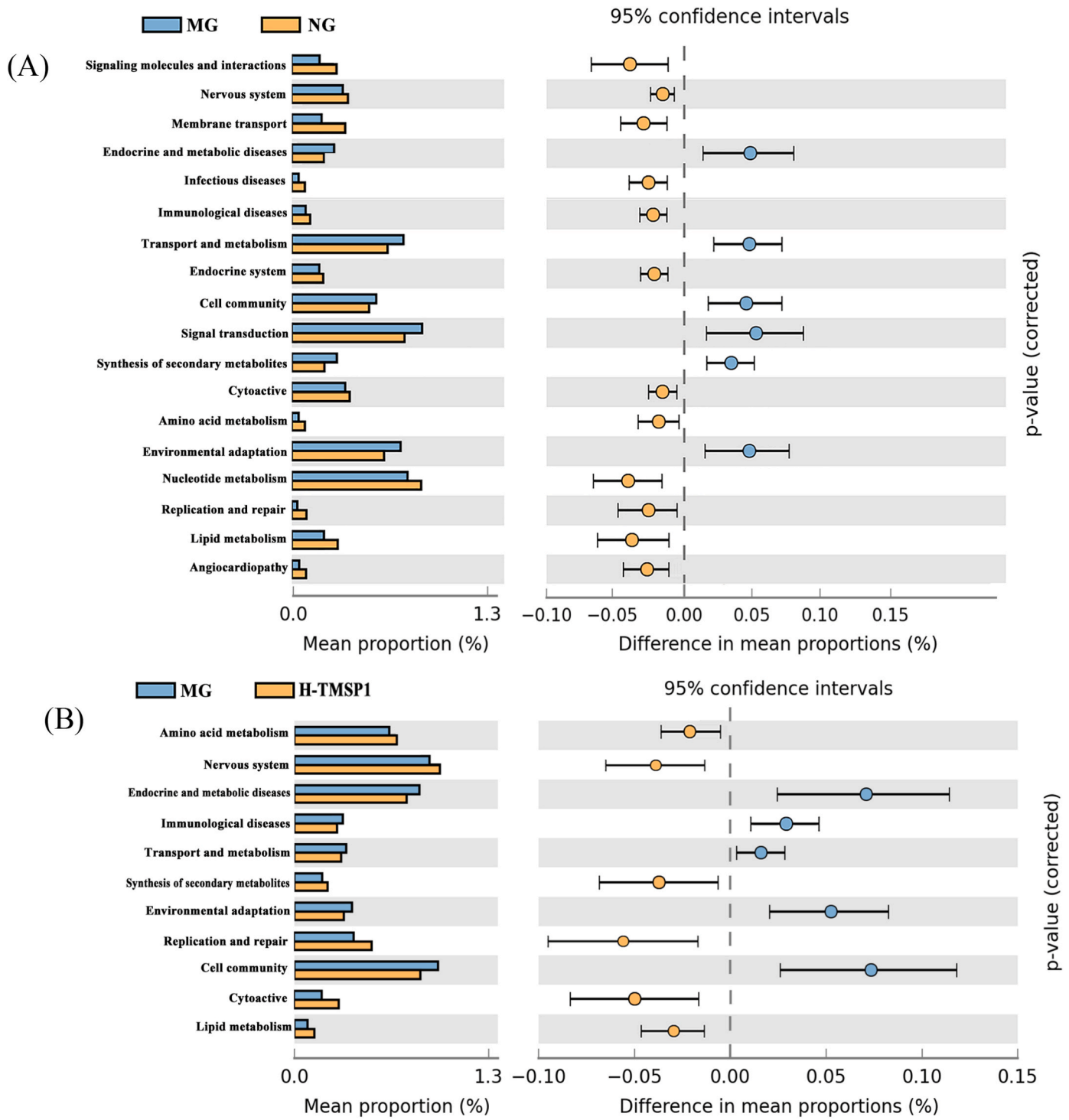

Fig. 17. Effects of (A) STZ and (B) H-TMSP1 on functional abundance of intestinal flora in mice. Each group of mice was given the corresponding dose of TMSP1 for 6 weeks. (TMSP1: *Trichosanthes kirilowii M*axim. homogeneous polysaccharide, NG: normal group, MG: mellitus control group, H-TMSP1: high dose TMSP1).

accumulation, ameliorated gut microbiota dysbiosis by increasing SCFAs-producing bacteria and mitigated intestinal inflammation and oxidative stress, and restored the integrity of the intestinal epithelial barrier and mucus barrier. At rhe same time, TMSP1 exerted hypoglycemic effect through regulating intestinal flora to a certain extent. In summary, this study provides a new understanding of the hpyerglycemic mechanism of polysaccharide, which provides a theoretical basis for the development of *Trichosanthes kirilowii* Maxim as a potential functional food. However, there are limitations in our study regarding the transformation of SCFA by gut microbiota and the hypoglycemic effects of different sources of *Trichosanthes kirilowii* Maxim polysaccharides. This study provided the preliminary work and reference for the development of *Trichosanthes kirilowii* Maxim polysaccharide as a functional food for hypoglycemia.

CRediT authorship contribution statement

Qiaoying Song: Data curation, Formal analysis, Methodology,

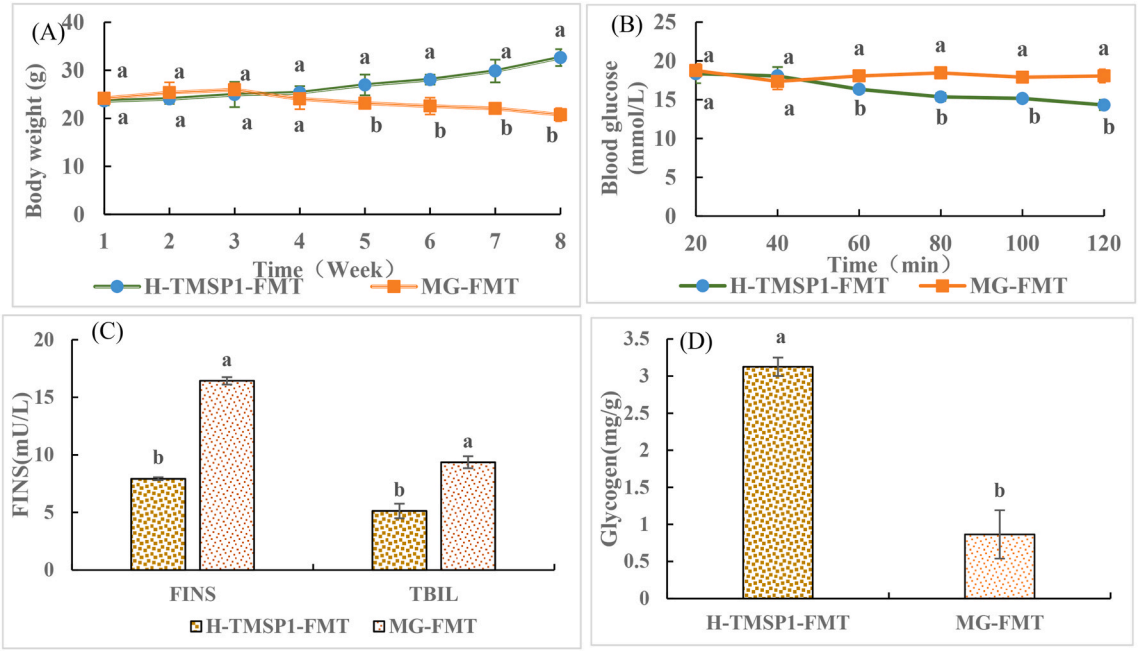

Fig. 18. Effect of FMT on serum biochemical in receipt mice. (A) The body weight levels, (B) Blood glucose, (C) FINS and TBIL, (D) Glycogen in H-TMSP1-FMT group and MG-FMT group. All mice were accommodated for one week and subsequently administered antibiotics (rifaximin, 150 mg/kg/day) for an additional daily for 2 weeks. The isolated fecal samples from H-TMSP1 group were and administered to recipient mice once daily for 8 weeks. Data are expressed as the means ± SEM (n = 10). Values with different letters are significantly different ($P < 0.05$). (TMSP1: *Trichosanthes kirilowii M*axim. homogeneous polysaccharide, NG: normal group, MG: mellitus control group, H-TMSP1: high dose TMSP1, FMT: fecal microbiota transplantation, FIns: fasting insulin, TBIL:Total Bilirubin).

Project administration, Conceptualization, Writing – original draft, Writing – review & editing. **Kunpeng Zhang:** Funding acquisition, Project administration, Supervision, Validation. **Shuyan Li:** Investigation, Project administration, Software, Supervision, Visualization. **Shaoting Weng:** Project administration, Supervision, Visualization, Data curation, Formal analysis, Investigation.

Declaration of competing interest

The authors declare that they have no known competing financial interests or personal relationships that could have appeared to influence the work reported in this paper.

Acknowledgements

This work was financially supported by technological program of Anyang,china (2022A02NY002); the Postdoctoral Innovation and Practice Base of Anyang Institute of Technology (BHJ2022010); the Staring Foundation for the Doctor Anyang Institute of Technology (BSJ2021026).

Appendix A. Supplementary data

Supplementary data to this article can be found online at https://doi.org/10.1016/j.crfs.2025.100977.

Data availability

Data will be made available on request.

References

Abbou, A., Kadri, N., Debbache, N., et al., 2019. Effect of precipitation solvent on some biological activities of polysaccharides from Pinus halepensis Mill. seeds. Int. J. Biol. Macromol. 141 (1), 663–670.
Almugadam, B.S., Yang, P., Tang, L., 2021. Analysis of jejunum microbiota of HFD/STZ diabetic rats. Biomed. Pharmacother. 138, 111094.
Bao, K., Belibasakis, G.N., Thurnheer, T., et al., 2014. Role of Porphyromonas gingivalis gingipains in multi-species biofilm formation. BMC Microbiol. 14 (1), 1–8.
Barbosa, J., Junior, R., 2021. Polysaccharides obtained from natural edible sources and their role in modulating the immune system: biologically active potential that can be exploited against COVID-19. Trends Food Sci. Technol. 108, 223–235.
Brian K, A., Cai, J.Y., Armstrong, J., et al., 2005. EF24, a novel synthetic curcumin analog, induces apoptosis in cancer cells via a redox-dependent mechanism. Anti Cancer Drugs 16 (3), 263–275.
Caporaso, J.G., Kuczynski, J., Stombaugh, J., et al., 2010. QIIME allows analysis of high-throughput community sequencing data. Nat. Methods 5, 335–336.
Cardullo, N., Muccilli, V., Pulvirenti, L., et al., 2020a. C-glucosidic ellagitannins and galloylated glucoses as potential functional food ingredients with anti-diabetic properties: a study of α-glucosidase and α-amylase inhibition. Food Chem. 313 (30), 126099.
Cardullo, N., Muccilli, V., Pulvirenti, L., et al., 2020b. C-glucosidic ellagitannins and galloylated glucoses as potential functional food ingredients with anti-diabetic properties: a study of α-glucosidase and α-amylase inhibition. Food Chem. 313 (30), 126099.
Chen, D., Ding, Y., Ye, H., et al., 2020a. Effect of long-term consumption of tea (Camellia sinensis L.) flower polysaccharides on maintaining intestinal health in BALB/c mice. J. Food Sci. 85 (6), 1948–1955.
Chen, H.H., Nie, Q.X., Hu, J.L., et al., 2020b. Metabolism amelioration of Dendrobium officinale polysaccharide on type II diabetic rats. Food Hydrocolloids 102, 105582.
Chen, D., Ding, Y., Ye, H., et al., 2020c. Effect of long-term consumption of tea (Camellia sinensis L.) flower polysaccharides on maintaining intestinal health in BALB/c mice. J. Food Sci. 85 (44), 1948–1955.
Chen, G.J., Chen, D., Zhou, W.T., et al., 2021. Improvement of metabolic syndrome in high-fat diet-induced mice by yeast β-glucan is linked to inhibited proliferation of Lactobacillus and Lactococcus in gut microbiota. J. Agric. Food Chem. 69 (27), 7581–7592.
Chen, S.T., Wang, M., Veeraperumal, S., et al., 2023a. Antioxidative and protective effect of Morchella esculenta against dextran sulfate sodium-induced alterations in liver. Foods 12 (5), 1115.
Chen, L.G., Shen, L., Zhu, L.Y., et al., 2023b. Hyperglycemia symptom amelioration by Ascophyllum nodosum polysaccharides in mice with type 2 diabetes. Algal Res. 75, 103278.
Cheng, Y., Yu, S., Xue, F., 2020. Puerariae lobatae comparison of the extraction efficiency of Isoflavone compounds from by ionic liquids with 11 anions and 8 imidazoliumbased cations. ACS Omega 5 (15), 8962–8971.
Chiang, J.Y., 2009. Bile acids: regulation of synthesis. JLR (J. Lipid Res.) 50 (10), 1955–1966.
Duan, Y., Young, R., Schnabl, B., 2022. Bacteriophages and their potential for treatment of gastrointestinal diseases. Nat. Rev. Gastroenterol. Hepatol. 19 (2), 135–144.
Fan, J., Feng, H.B., Yu, Y., et al., 2017a. Antioxidant activities of the polysaccharides of Chuanminshen violaceum. Carbohydr. Polym. 157 (10), 629–636.
Fan, J., Feng, H.B., Yu, Y., et al., 2017b. Antioxidant activities of the polysaccharides of Chuanminshen violaceum. Carbohydr. Polym. 157 (10), 629–636.

Fu, W., Wu, R., Wan, M., et al., 2021. Hypoglycemic and hypolipidemic effects of non-starch polysaccharide from Dolichos Lablab L in type II diabetic rats. Mod. Food Sci. Technol. 37 (8), 1–7.
Gill, S.R., Pop, M., Deboy, R.T., et al., 2006. Metagenomic analysis of the human distal gut microbiome. Science 312 (5778), 1355–1359.
Giuliano, A.R., Nyitray, A.G., Kreimer, A.R., et al., 2015. EUROGIN 2014 roadmap: differences in human papillomavirus infection natural history, transmission and human papillomavirus-related cancer incidence by gender and anatomic site of infection. Int. J. Cancer 36, 2752–2760.
Goyal, S.N., Reddy, N.M., Patil, K.R., et al., 2016. Challenges and issues with streptozotocin-induced diabetes-a clinically relevant animal model to understand the diabetes pathogenesis and evaluate therapeutics. Chem. Biol. Interact. 244 (25), 49–63.
Guan, Z.F., Zhou, X.L., Zhang, X.M., et al., 2016. Beclin-1- mediated autophagy may be involved in the elderly cognitive and affective disorders in streptozotocin-induced diabetic mice. Transl. Neurodegener. 5 (1), 22.
Habib, H.M., Theuri, S.W., Kheadr, E.E., et al., 2017. Functional, bioactive, biochemical, and physicochemical properties of the Dolichos lablab bean. Food Funct. 8 (2), 872–880.
Hu, R.K., Zeng, F., Wu, L., et al., 2019. Fermented carrot juice attenuates type 2 diabetes by mediating gut microbiota in rats. Food Funct. 10 (5), 2935–2946.
Hu, Z.Y., Zhou, H.L., Zhao, J.L., et al., 2020. Microwave-assisted extraction, characterization and immunomodulatory activity on RAW264.7 cells of polysaccharides from Trichosanthes kirilowii Maxim seeds. Int. J. Biol. Macromol. 164, 2861–2872.
Huang, L.T., Yang, Z., Yuan, J.K., et al., 2023. Preparation and characteristics of pumpkin polysaccharides and their effects on abnormal glucose metabolism in diabetes mice. Food Biosci. 54, 102792.
Jing, Y., Cao, R.X., Lei, X., et al., 2024. Structural characterization of polysaccharide from the peel of Trichosanthes kirilowii Maxim and its anti-hyperlipidemia activity by regulating gut microbiota and inhibiting cholesterol absorption. Bioorg. Chem. 149, 107487.
Kyrgiou, M., Mitra, A., Moscicki, A.B., 2017. Does the vaginal microbiota play a role in the development of cervical cancer. Transl. Res. 179, 168–182.
Lang, X.S.J., Zhao, N., He, Q., et al., 2020. Treadmill exercise mitigates neuroinflammation and increases BDNF via activation of SIRT1 signaling in a mouse model of T2DM. Brain Res. Bull. 165, 30–39.
Li, J.C., Huang, G.L., 2021. Extraction, purification, separation, structure, derivatization and activities of polysaccharide from Chinese date. Process Biochem. 110, 231–242.
Li, Y., Xu, S.Q., Mihaylova, M.M., et al., 2011. AMPK phosphorylates and inhibits SREBP activity to attenuate hepatic steatosis and atherosclerosis in diet-induced insulinresistant mice. Cell Metabol. 13 (4), 376–388.
Li, B.X., Liang, F., Ding, X.Y., et al., 2019. Interval and continuous exercise overcome memory deficits related to beta-Amyloid accumulation through modulating mitochondrial dynamics. Behav. Brain Res. 376 (30), 112–171.
Li, F., Wei, Y.L., Liang, L., et al., 2021. A novel low-molecular-mass pumpkin polysaccharide: structural characterization, antioxidant activity, and hypoglycemic potential. Carbohydr. Polym. 251, 117090.
Li, X.L., Ma, R.H., Zhang, F., et al., 2023. Evolutionary research trend of Polygonatum species: a comprehensive account of their transformation from traditional medicines to functional foods. Crit. Rev. Food Sci. Nutr. 63 (19), 3803–3820.
Liang, Z.R., Li, D.W., Peng, S.M., 2009. Effects of seed extracts from Trichosanthes kirilowii Maxim on antifeeding and growth and development of Pieris rapae L. N. Biotech. 25, S251.
Liang, L., Liu, G.M., Yu, G.Y., et al., 2020. Urinary metabolomics analysis reveals the anti-diabetic effect of stachyose in high-fat diet/streptozotocininduced type 2 diabetic rats. Carbohydr. Polym. 229, 115534.
Liu, H.X., Kwame Amakye, W., Ren, J.Y., 2021a. Codonopsis pilosula polysaccharide in synergy with dacarbazine inhibits mouse melanoma by repolarizing M2-like tumor-associated macrophages into M1-like tumor-associated macrophages. Biomed. Pharmacother. 142, 112016.
Liu, J.F., Pu, Q.S., Qiu, H.D., et al., 2021b. Polysaccharides isolated from Lycium barbarum L. by integrated tandem hybrid membrane technology exert antioxidant activities in mitochondria. Ind. Crop. Prod. 168 (15), 113547.
Liu, J.S., Liu, Y., Sun, J., et al., 2023. Protective effects and mechanisms of Momordica charantia polysaccharide on early-stage diabetic retinopathy in type 1 diabetes. Biomed. Pharmacother. 168, 115726.
Liu, T.T., Zhao, M., Zhang, Y.M., et al., 2024. Polysaccharides from Phellinus linteus attenuate type 2 diabetes mellitus in rats via modulation of gut microbiota and bile acid metabolism. Int. J. Biol. Macromol. 262 (1), 130062.
Lu, X.Y., Dong, Y.Q., Jian, Z.C., et al., 2019. Systematic investigation of the effects of long-term administration of a high-fat diet on drug transporters in the mouse liver, kidney and intestine. Curr. Drug Metabol. 20 (9), 742–755.
Lunken, G.R., Tsai, K., Schick, A., et al., 2021. Prebiotic enriched exclusive enteral nutrition suppresses colitis via gut microbiome modulation and expansion of anti-inflammatory T cells in a mouse model of colitis. Cell. Mol. Gastroenterol. Hepatol. 12 (4), 1251–1266.
Miao, Y., Guo, D.H., Li, W., et al., 2019. Diabetes promotes development of Alzheimer's disease through suppression of autophagy. J. Alzheim. Dis. 69 (1), 289–296.
Moheet, A., Mangia, S., Seaquist, E.R., 2015. Impact of diabetes on cognitive function and brain structure. Ann. N. Y. Acad. Sci. 1353, 60–71.
Moon, S.S., Rahman, A.A., Kim, J.Y., et al., 2008. Hanultarin, a cytotoxic lignan as an inhibitor of actin cytoskeleton polymerization from the seeds of Trichosanthes kirilowii. Bioorg. Med. Chem. 16 (15), 7264–7269.
Plovier, H., Everard, A., Druart, C., et al., 2016. A purified membrane protein from Akkermansia muciniphila or the pasteurized bacterium improves metabolism in obese and diabetic mice. Nat. Med. 23 (1), 107–113.
Qin, J.J., Li, Y.R., Cai, Z.M., et al., 2012. A metagenome-wide association study of gut microbiota in type 2 diabetes. Nature 490 (7418), 55–60.
Qu, L., Ren, J.L., Huang, L., et al., 2018. Antidiabetic effects of Lactobacillus casei fermented yogurt through reshaping gut microbiota structure in type 2 diabetic rats. J. Agric. Food Chem. 66 (48), 12696–12705.
Rahman, A.A., Moon, S.S., 2007. Isoetin 5'-methyl ether, a cytotoxic flavone from Trichosanthes kirilowii. J. Cheminf. 28 (8), 1261–1264.
Ribovski, L., Jong, E.D., Mergel, O., et al., 2021. Low nanogel stiffness favors nanogel transcytosis across an in vitro blood-brain barrier. Nanomed. Nanotechnol. Biol. Med. 34, 102377.
Rognes, T., Flouri, T., Nichols, B., et al., 2016. VSEARCH: a versatile open source tool for metagenomics. PeerJ 4, e2584.
Sanna, S., van Zuydam, N.R., Mahajan, A., et al., 2019. Causal relationships among the gut microbiome, short-chain fatty acids and metabolic diseases. Nat. Genet. 51 (4), 600–605.
Shen, N., Jiang, S., Lu, J.M., et al., 2015. The constitutive activation of Egr-1/C/EBPa mediates the development of type 2 diabetes mellitus by enhancing hepatic gluconeogenesis. Am. J. Pathol. 185 (2), 513–523.
Shu, S.H., Xie, G.Z., Guo, X.L., et al., 2009. Purification and characterization of a novel ribosome-inactivating protein from seeds of Trichosanthes kirilowii Maxim. Protein Expr. Purif. 67 (2), 120–125.
Su, L., Xin, C.X., Yang, J.T., et al., 2022. A polysaccharide from Inonotus obliquus ameliorates intestinal barrier dysfunction in mice with type 2 diabetes mellitus. Int. J. Biol. Macromol. 214 (1), 312–323.
Tong, K.I., Katoh, Y., Kusunoki, H., 2006. Keap1 recruits Neh2 through binding to ETGE and DLG motifs:characterization of the two-site molecular recognition model. Mol. Cell Biol. 26, 2887–2900.
Wang, H.Y., Zhao, M.M., Yang, B., et al., 2007. Identification of polyphenols in tobacco leaf and their antioxidant and antimicrobial activities. Food Chem. 107 (4), 1399–1406.
Wang, W.F., Wang, L.Z., Jiang, J.X., 2009. Fatty acid profile of Trichosanthes kirilowii Maxim. seed oil. Nephron Clin. Pract. 63 (4), 489–492.
Wang, L.Q., Xu, N., Zhang, J.J., et al., 2015. Antihyperlipidemic and hepatoprotective activities of residue polysaccharide from Cordyceps militaris SU-12. Carbohydr. Polym. 131, 355–362.
Wang, N.N., Liu, Y., Ma, Y.N., et al., 2017. High-intensity interval versus moderateintensity continuous training: superior metabolic benefits in diet-induced obesity mice. Life Sci. 191, 122–131.
Wang, X.Y., Zhang, D.D., Yin, J.Y., et al., 2019. Recent developments in Hericium erinaceus polysaccharides: extraction, purification, structural characteristics and biological activities. Crit. Rev. Food Sci. Nutr. 59, S96–S115.
Wang, S.N., Qu, D.N., Zhao, G.L., et al., 2022a. Characterization of the structure and properties of the isolating interfacial layer of oil-water emulsions stabilized by soy hull polysaccharide: effect of pH changes. Food Chem. 370 (15), 131029.
Wang, R., Shan, H.L., Zhang, G.J., et al., 2022b. An inulin-type fructan (AMP1-1) from Atractylodes macrocephala with anti-weightlessness bone loss activity. Carbohydr. Polym. 294 (15), 119742.
Wu, Q.Q., Wang, Q.T., Fu, J.F., et al., 2019. Polysaccharides derived from natural sources regulate triglyceride and cholesterol metabolism: a review of the mechanisms. Food Funct. 10 (5), 2330–2339.
Wu, Z.H., Huang, S.M., Li, T.T., et al., 2021. Gut microbiota from green tea polyphenol-dosed mice improves intestinal epithelial homeostasis and ameliorates experimental colitis. Microbiome 9 (1), 184.
Wu, R.T., Wang, L.F., Yao, Y.F., et al., 2022a. Activity fingerprinting of polysaccharides on oral, gut, pancreas and lung microbiota in diabetic rats. Biomed. Pharmacother. 155, 113681.
Wu, J., Jia, R.B., Luo, D.H., et al., 2022b. Sargassum fusiforme polysaccharide is a potential auxiliary substance for metformin in the management of diabetes. Food Funct. 13 (5), 3023–3035.
Wu, Y., Li, A., Liu, H., et al., 2022c. Lactobacillus plantarum HNU082 alleviates dextran sulfate sodium-induced ulcerative colitis in mice through regulating gut microbiome. Food Funct. 13 (19), 10171–10185.
Xia, B., Wu, W., Zhang, L., et al., 2021. Gut microbiota mediates the effects of inulin on enhancing sulfomucin production and mucosal barrier function in a pig model. Food Funct. 12 (21), 10967–10982.
Yan, J.M., Meng, Y., Zhang, M.S., et al., 2019. A 3-O-methylated heterogalactan from Pleurotus eryngii activates macrophages. Carbohydr. Polym. 206 (15), 706–715.
Yi, Y., Hua, H.M., Sun, X.F., et al., 2020. Rapid determination of polysaccharides and antioxidant activity of Poria cocos using near-infrared spectroscopy combined with chemometrics. Spectrochim. Acta Part A-molecular and Biomolecular Spectroscopy 240, 118623.
Zeng, F.S., Yao, Y.F., Wang, L.F., et al., 2023. Polysaccharides as antioxidants and prooxidants in managing the double-edged sword of reactive oxygen species. Biomed. Pharmacother. 159, 114221.
Zhan, M., Liang, X., Chen, J., et al., 2023. Dietary 5-demethylnobiletin prevents antibiotic-associated dysbiosis of gut microbiota and damage to the colonic barrier. Food Funct. 14 (9), 4414–4429.
Zhang, W.J., Wang, J.Y., Chen, Y.S., et al., 2020a. Flavonoid compounds and antibacterial mechanisms of different parts of white guava (Psidium guajava L. cv. Pearl). Nat. Prod. Res. 34 (11), 1621–1625.
Zhang, W.J., Xiang, Q.F., Zhao, J., et al., 2020b. Purification, structural elucidation and physicochemical properties of a polysaccharide from Abelmoschus esculentus L (okra) flowers. Int. J. Biol. Macromol. 155, 740–750.

Zhou, T., Jiang, Y.M., Wen, L.R., et al., 2021. Characterization of polysaccharide structure in Citrus reticulate 'Chachi' peel during storage and their bioactivity. Carbohydr. Res. 508, 108398.
Zhou, N., Zhao, Y., Zhang, L.G., et al., 2022a. Protective effects of black onion polysaccharide on liver and kidney injury in T2DM rats through the synergistic impact of hypolipidemic and antioxidant abilities. Int. J. Biol. Macromol. 223 (31), 378–390.
Zhou, W.T., Yang, T.T., Xu, W.Q., et al., 2022b. The polysaccharides from the fruits of Lycium barbarum L. confer anti-diabetic effect by regulating gut microbiota and intestinal barrier. Carbohydr. Polym. 291, 119626.